

Advances in Soft Mechanocaloric Materials

Xiujun Fan, Songyue Chen, Farid Manshahi, Zhaoqi Duan, Guorui Chen, Xun Zhao, Yihao Zhou, and Jun Chen*

The development of soft mechanocaloric materials is becoming increasingly important due to the growing demand for energy-efficient and environmentally friendly thermoregulation solutions. Here the mechanocaloric effects in soft materials, which can convert mechanical energy into heat energy, is discussed, and their applications in sensing, therapeutics, and thermoregulation is explored. It begins by introducing the principles of the mechanocaloric effect and recent advances in its study within soft materials' systems. Then applications of mechanocaloric effects in personalized healthcare and sustainable energy is explored. Finally, the importance of identifying soft materials with high mechanocaloric coefficients and low manufacturing costs is emphasized to broaden their applicability. Additionally, a comprehensive perspective on mechanocaloric effects is provided for both heating and cooling applications, emphasizing the transformative potential of soft mechanocaloric materials in various fields.

1. Introduction

Humans, as homeothermic beings, rely significantly on the efficiency of our bodies' energy conversion systems to maintain a stable internal temperature. For instance, in cold environments, shivering and the metabolic breakdown of glucose through glycolysis can collectively generate between 2000 and 2500 calories per day. This energy output is equivalent to powering a 50 W light bulb for over 45 h. On the one hand, body thermal energy harvesting is a popular approach toward personalized healthcare and sustainable energy.^[1–4] Meanwhile, body thermoregulation occurs in nature, exemplified by the magnetocaloric effect, where significant temperature changes arise when materials are exposed to magnetic fields.^[5] These phenomena could be harnessed to enhance energy efficiency and promote sustainability.

Despite technological advancements, thermoregulation—particularly methods that rely on outdated technologies—continues to present sustainability challenges.^[6–8] For example, refrigeration accounts for 20–30% of global electricity consumption. Moreover, traditional gas compression technologies, which utilize hydrofluorocarbon compounds (such as Freon

and HCFCs), not only severely damage the ozone layer but also contribute significantly to global warming. In contrast, solid-state thermoregulation technologies generally provide a higher coefficient of performance (COP) compared to conventional systems, allowing for efficient cooling even at lower temperature differentials.^[9–11]

Amid these challenges, mechanocaloric technology has emerged as a promising thermoregulation method. This innovative approach induces phase transitions in materials through external forces, inducing substantial thermal fluctuations. When subjected to stress, mechanocaloric materials undergo transformations that modify their internal structure and energy state, resulting in notable thermal variations. During cycles of stress application and release, these materials typically absorb

energy when under stress and release it upon returning to their original state. It is important to note that the mechanical forces applied must be sufficient to overcome the phase transformation barriers, such as the transition from martensite to austenite.^[12] A key challenge in mechanocaloric technology is the phenomenon of hysteresis, similar to the hysteresis curve that describes the lag in magnetization after exposure to a magnetic field. In mechanocaloric materials, hysteresis refers to the energy loss that occurs during mechanical loading and unloading cycles. This phenomenon prevents the material from fully recovering its original state during pressure changes, thereby affecting the conversion efficiency of the thermal effect and the energy storage and release processes. Such an energy loss significantly impacts the efficiency of the mechanocaloric effect, especially during rapid cycles, as the material's energy loss cannot be fully converted into temperature changes in each loading and unloading cycle. This limitation further restricts its performance in practical applications. Therefore, identifying and optimizing materials with low hysteresis is crucial to enhancing the overall energy conversion efficiency of mechanocaloric technologies. This review primarily focuses on minimizing hysteresis through material selection, aiming to enhance the thermoregulation efficiency and practical applicability of the mechanocaloric effect.^[13]

Another challenge is that current thermal energy harvesting devices are predominantly constructed using metal systems, primarily shape memory alloys (SMAs) such as Ni–Ti and Cu–Zn–Al,^[14] as well as magnetic shape memory alloys.^[15] Although these alloys can produce significant adiabatic temperature changes, sometimes exceeding 20 K,^[16,17] their high Young's modulus renders them incompatible with biological tissues,

X. Fan, S. Chen, F. Manshahi, Z. Duan, G. Chen, X. Zhao, Y. Zhou, J. Chen
Department of Bioengineering
University of California, Los Angeles
Los Angeles, California 90095, USA
E-mail: jun.chen@ucla.edu

 The ORCID identification number(s) for the author(s) of this article can be found under <https://doi.org/10.1002/adfm.202420997>

DOI: 10.1002/adfm.202420997

thereby limiting their application in soft bioelectronics.^[18,19] Luckily, recent discoveries indicate that the mechanocaloric effect can also occur in soft systems, such as elastomers and polymers. This development opens up new opportunities for designing smart textiles that leverage the elastocaloric effect.^[20] Besides, innovations like active cooling textiles, thermoelectric units, nanoporous metalized polyethylene fabric, and moisture transport fabrics all play a significant role in thermal management in everyday life.^[6–8] Similar to the transition from martensite to austenite, which involves distinct energy states, soft systems undergo varying internal energy conditions, resulting in warming or cooling during these transitions.^[11]

In addition to these advancements, considerable efforts have been directed toward the exploration of novel materials for thermoregulation and the investigation of their underlying fundamental sciences. For instance, a recently developed class of mechanocaloric materials can convert mechanical energy obtained from various forms of applied force—such as tension, compression, and torsion.^[9–11] This leads to alterations in the material's internal structure or phase transformation. These phenomena are commonly referred to as the elastocaloric effect, the barocaloric effect (BCE), and the twistocaloric effect. Additionally, the integration of 2D materials has significantly enhanced heat conductivity properties. These strategies indicate a promising path toward a sustainable energy future.

In this review, we primarily focus on the mechanocaloric effect in soft materials' systems, particularly in the contexts of therapeutics and thermoregulation. We begin by examining the principles of the mechanocaloric effect and then transition to the discovery of this phenomenon in soft systems. We then examine the current applications of the mechanocaloric effect in soft systems within personalized healthcare and energy sectors. Finally, we emphasize the importance of identifying soft materials with high mechanocaloric coefficients and low manufacturing costs to broaden their applicability. This advancement would not only support green energy initiatives but also address issues related to the low heat conversion efficiency and durability of mechanocaloric soft materials under repeated stretching and compression cycles.

2. Principles of Mechanocaloric Effect

The mechanocaloric effect was first discovered in rigid metal systems, leading to the development of well-established theories that explain its mechanisms. This effect includes both warming and cooling processes, which together form a cycle typically referred to as endothermic and exothermic circulation. In an endothermic process, the material absorbs heat from its surroundings during deformation. This generally occurs when the material is subjected to tensile stress, leading to a phase transformation, such as the transition from austenite to martensite in SMAs. As the material deforms, energy is required to facilitate the phase transformation, resulting in a decrease in temperature. Conversely, during unloading or compression in an exothermic process, the material releases heat to its surroundings.^[21,22] This energy release causes an increase in temperature, which can be advantageous in applications where heat generation is desired (Figure 1a).

Rigid systems exhibiting the mechanocaloric effect, such as SMAs and ferroelectric materials, consist of a crystal lattice.

When mechanical forces are applied, these forces act as a catalyst for the transformation from a parent crystal structure to a product crystal structure. Initially, the lattice is organized in a regular 3D arrangement. However, when external forces exceed the lattice energy, deformation occurs.^[23] In contrast, soft systems such as polymers do not possess a crystal lattice but still require energy to overcome barriers for deformation.^[18,19,24–27] In mechanocaloric polymer materials, the polymers are typically arranged in an amorphous (noncrystalline) state under no stress. However, when subjected to stress, they reorganize to form crystalline domains. This process is known as strain-induced crystallization (SIC). These changes enhance the strength and toughness of the materials, enabling them to recover their original shape after the load is removed (Figure 1b). However, traditional polymers are formed through random crosslinking processes, resulting in trapped entanglements and inhomogeneities. These factors increase the minimum force required for SIC and reduce its overall extent. To address this limitation, a novel approach involves constructing a deswollen end-linked star elastomer system with a homogeneous architecture. This configuration facilitates improved chain alignment during stretching (Figure 1b).^[28]

The extent of the mechanocaloric effect is governed by the Clausius–Clapeyron equation, as shown in Equation (1). This equation describes the relationship between the pressure and temperature of a substance during a phase transition—such as between liquid and vapor (boiling) or solid and liquid (melting)—based on thermodynamic principles.^[17] Materials can exist in two phases depending on their levels of structural symmetry. When a transition occurs between these two phases, the stress–temperature response changes. A stress–temperature diagram is used to specifically characterize the temperature change cycle during phase transitions (Figure 1c). Due to the phase transition of a material's thermodynamic state (such as changes in lattice structure or crystallized regions), energy barriers are overcome, shifting the equilibrium point. This is also evident in the changes to the entropy–temperature relationship during the phase transition. As a result, mechanical forces can influence the material's entropy, and when a phase change occurs, the temperature change cycle is directly affected (Figure 1d):

$$\frac{dP}{dT} = \frac{\Delta H}{T\Delta V} \quad (1)$$

where P is the pressure, T is the temperature, ΔH is the enthalpy change during the phase transition, and ΔV is the volume change during the phase transition. This formulation of the Clausius–Clapeyron equation highlights the relationship between enthalpy change and temperature during a phase transition.

It is also important to note that a material's response to mechanical stress during a phase transition is path dependent, a phenomenon known as hysteresis (Figure 1e). The stress–strain graph forms a loop, and the area enclosed by this hysteresis loop represents energy losses due to internal friction and other dissipative processes during the phase transition. These losses can decrease the efficiency of cooling systems that utilize the mechanocaloric effect. Furthermore, the presence of the hysteresis loop indicates that a material may remain in a high-temperature phase even after the stress is reduced, especially if it has previously been subjected to high stress. Therefore,

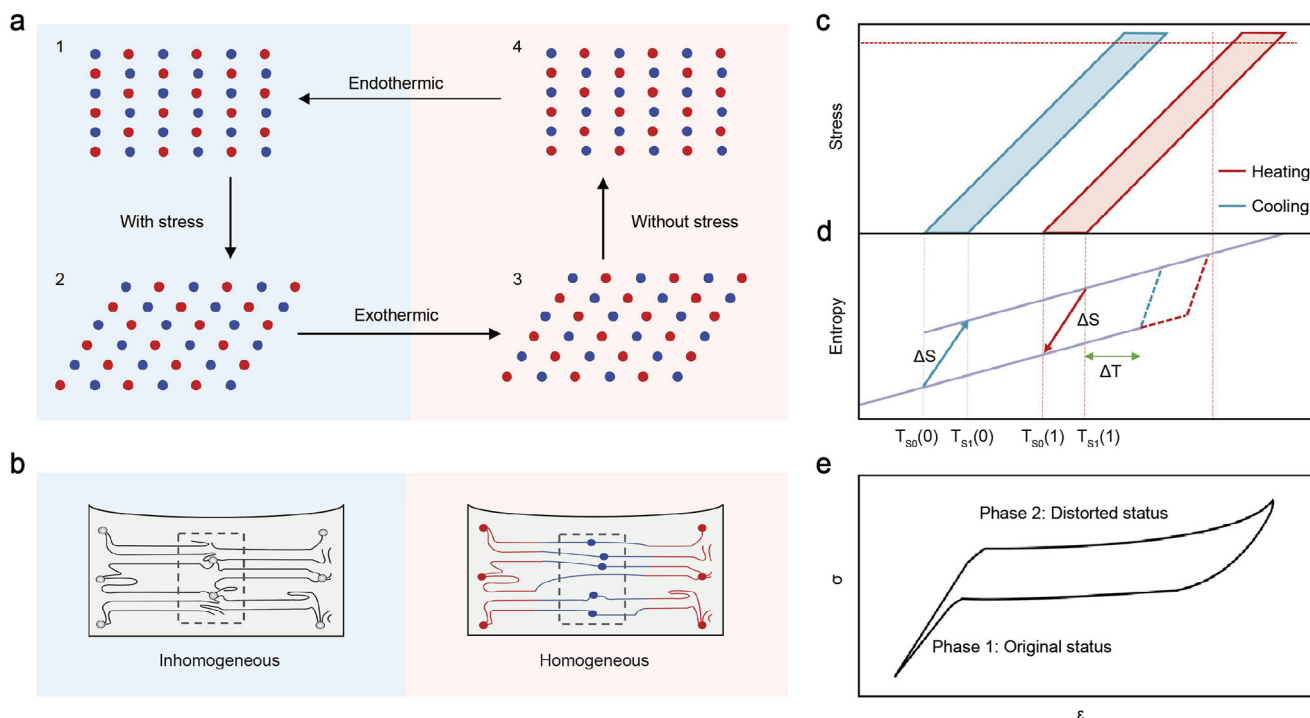


Figure 1. Principles of the mechanocaloric effect. a) Endothermic and exothermic circulation in rigid systems: 1) beginning state, 2) application of stress, with pressure release as an exothermic phenomenon, 3) pressure release, and 4) after returning to its original state, the material absorbs heat. b) Strain-induced crystallization (SIC) in elastomers. Left: Physical barriers like trapped entanglements negatively impact SIC. Right: Homogeneous architecture initiates SIC. Reproduced with permission.^[28] Copyright 2023, American Association for the Advancement of Science. c) Stress and temperature relationship based on the Clausius–Clapeyron equation. Reproduced with permission.^[11] Copyright 2022, Springer Nature. d) Entropy changes during temperature increase and decrease cycles. Two purple lines indicate heating and cooling, marked as red and blue cycles, respectively. Reproduced with permission.^[33] Copyright 2021, Springer Nature. e) Applied stress (σ) versus strain (ϵ) changes between two states. Reproduced with permission.^[11] Copyright 2022, Springer Nature.

optimizing materials to achieve a smaller hysteresis loop is crucial for enhancing the performance of thermoregulation, as it can help enhance energy saving and improve overall system efficiency.^[29]

Therefore, mechanocaloric effects refer to the phenomenon where structural changes and accompanying temperature variations occur in materials under external mechanical stimuli. The main mechanocaloric effects include elastocaloric, twistocaloric, and barocaloric effects. The elastocaloric effect involves deforming the material by applying uniaxial stress, leading to structural changes or phase transitions within the material, resulting in temperature changes. In contrast, the twistocaloric effect relies on the torsional deformation of the material, i.e., applying a rotational strain to deform the material, which in turn triggers a change in temperature. Lastly, the barocaloric effect induces phase transitions or structural transformations in the material by applying or releasing pressure, leading to heat absorption or release.^[28–31]

These three effects differ significantly in their mechanisms. The elastocaloric effect primarily relies on deformation and phase changes induced by uniaxial stress, typically occurring in simpler stress states. The twistocaloric effect emphasizes deformation under torsion. Compared to the uniaxial stress of the elastocaloric effect, the torsional strain involves more complex mechanical operations and exhibits distinct temperature change

characteristics. On the other hand, the barocaloric effect regulates temperature through pressure changes and usually involves phase transitions or crystallization processes in the material. Section 3 will further explore how these three effects perform, analyzing their respective advantages and disadvantages to provide valuable insights for future research and applications.

3. Mechanocaloric Effects in Soft Materials' Systems

3.1. Elastocaloric Effect in Soft Materials' Systems

The elastocaloric effect refers to the temperature change that occurs in a material when it undergoes mechanical deformation. While this effect can also be observed in shape memory alloys, this section specifically focuses on its manifestation in polymers.

Unlike metals, which are composed of atoms arranged in a crystalline structure, many soft elastomers consist of amorphous chains. Under stress, these chains can align and reorganize, leading to crystallization. Energy changes occur during crystallization, leading to corresponding temperature changes. Three primary factors influence the efficiency of SIC. According to the Clausius–Clapeyron equation Equation (1), the temperature (T) at which deformation occurs can impact the crystallization process. Higher temperatures may enhance polymer chain

mobility, promoting crystallization. Strain rate measured by volume change (ΔV) represents the rate at which the material is deformed and influences the crystallization process. Faster deformation can increase the rate of the crystallization process. The composition of the polymer, including its chemical structure and molecular weight, impacts the enthalpy change (ΔH) during crystallization. Therefore, different polymers and copolymers exhibit varying tendencies for SIC.^[28–30]

To optimize a material for the elastocaloric effect, it is crucial to perform mechanical testing to determine the elastic deformation ranges, thermal analysis to evaluate heat flow during deformation, and phase transition analysis to identify phase transformation temperatures. Adjusting polymer composition—from single compositions such as natural rubber (NR), synthetic rubber, or thermoplastic elastomers (TPEs) to blends of different polymers, additives, or fillers—can achieve dual elasticity. Compared to conventional elastocaloric elastomers, dynamic elasticity and low stiffness elastomers (DELSE) exhibit lower stiffness and higher elasticity, enabling them to deform more easily under stress while returning to their original shape. This is attributed to DELSE's unique gelation process, which enables a more controlled and rapid transition from a liquid to a gel state, making it suitable for applications that require high flexibility and dynamic performance (Figure 2a,b). Temperature changes during adiabatic stretching, measured by an infrared camera, are three times greater than those observed in conventional elastocaloric elastomers (Figure 2c).^[28]

Furthermore, DELSE exhibits minimal stress–stretch hysteresis due to its dynamic crosslinking mechanism, which enables its internal structure to quickly revert to its original state, thus minimizing energy loss. The material's high elasticity and low stiffness facilitate easy deformation, resulting in lower energy dissipation during loading and unloading cycles. Notably, this low hysteresis remains stable even when the material is stretched to 12 times its original length ($\lambda = 12$, Figure 2d,e). A heat pump extracts heat from a source—such as air, ground, or water—and transfers it to a different location, typically against the natural flow of heat.^[31] Heat pumps operate using a refrigeration cycle consisting of four main components. The evaporator absorbs heat from the source (e.g., outdoor air) as the refrigerant evaporates. The compressor then compresses the refrigerant gas, which raises its pressure and temperature. The condenser releases the absorbed heat into the desired space (e.g., indoors) as the refrigerant condenses back into a liquid. The expansion valve then reduces the pressure of the refrigerant, allowing it to expand and cool before re-entering the evaporator.^[32]

Traditional heat transfer devices encounter significant challenges related to sustainable energy, and materials that exhibit the mechanocaloric effect are primarily rigid, which restricts their use in heat pumps. However, a novel soft system developed from natural rubber effectively combines SIC with snap-through instability. This phenomenon occurs in certain mechanical systems, where a nonlinear response to applied loads leads to a rapid change in configuration. This combination enables the material to demonstrate a fast transition rate with minimal energy loss. The elastocaloric modulus can be fabricated as a membrane structure, making it suitable for compact spaces (Figure 2f). Additionally, optimized rubber membranes facilitate the direct con-

version of electrical energy into low-noise pneumatic actuation (Figure 2g,h).^[33,34]

Enhancing energy conversion efficiency in the elastocaloric effect can be achieved through various strategies, including optimizing materials that exhibit greater entropy changes during deformation. This results in increased adiabatic temperature changes, contributing to significant thermoregulation in applications. For instance, polystyrene-*b*-poly(ethylene-*co*-butylene)-*b*-polystyrene has demonstrated exceptional elastocaloric performance. However, the presence of the ethyl side group restricts internal rotation and conformational changes. By reducing the ethyl group ratio from 33% to 8 mol%, the adiabatic temperature change increases from -4.3 to -16.3 K, and the isothermal entropy change increases from 38.5 to 173.3 J kg⁻¹ K⁻¹. Another improvement can be achieved through the use of advanced device designs. Kirigami structures, renowned for their stretchability and flexibility, offer significant advantages in harvesting mechanical energy. Due to the inherent anisotropy of these structures, they are well suited for versatile control of localized elastocaloric thermoregulation (Figure 2i).^[34]

It is important to note that the elastocaloric effect also occurs in isotropic materials, such as liquid crystalline elastomers (LCEs), which broadens its potential applications beyond solid-state systems and into soft materials and bioelectronics. The order–disorder transitions that occur during deformation disrupt the alignment of mesogenic segments, resulting in significant entropy changes. Compared to anisotropic LCEs, isotropic LCEs exhibit lower yield forces and can achieve temperature changes up to seven times greater than those of natural rubber, making them particularly promising for energy-efficient bioelectronic applications.^[35]

3.2. Barocaloric Effect in Soft Materials' Systems

In 2019, Li et al.^[36] reported on a class of disordered solids known as plastic crystals that exhibit a tremendously colossal barocaloric effect (CBCE). The barocaloric effect refers to the phenomenon in which a phase or structural transformation of a material, triggered by the application or release of pressure, leads to an entropic change that can absorb or release heat. This contrasts with the elastocaloric effect, which involves an entropic change due to a phase change or structural transformation when strain is applied or released, also resulting in the absorption or release of heat.

As an active barocaloric storage thermoregulation method, the BCE leverages the phase change processes that materials undergo in response to pressure changes—such as magnetic phase transitions and structural changes in solid-state materials—to absorb or release heat. This phase change thermal effect facilitates significant temperature changes during pressure variations, making it advantageous for cooling or heating applications. The barocaloric regenerative refrigeration cycle operates on a four-step thermodynamic process. Under adiabatic conditions, an increase in pressure results in a rise in temperature within the system. The heat transfer fluid is then directed to the warmer side at a constant pressure (P_2), resulting in cooling of the system. Under isentropic conditions, the system's temperature continues to decrease. Finally, the heat transfer fluid flows from the hot side

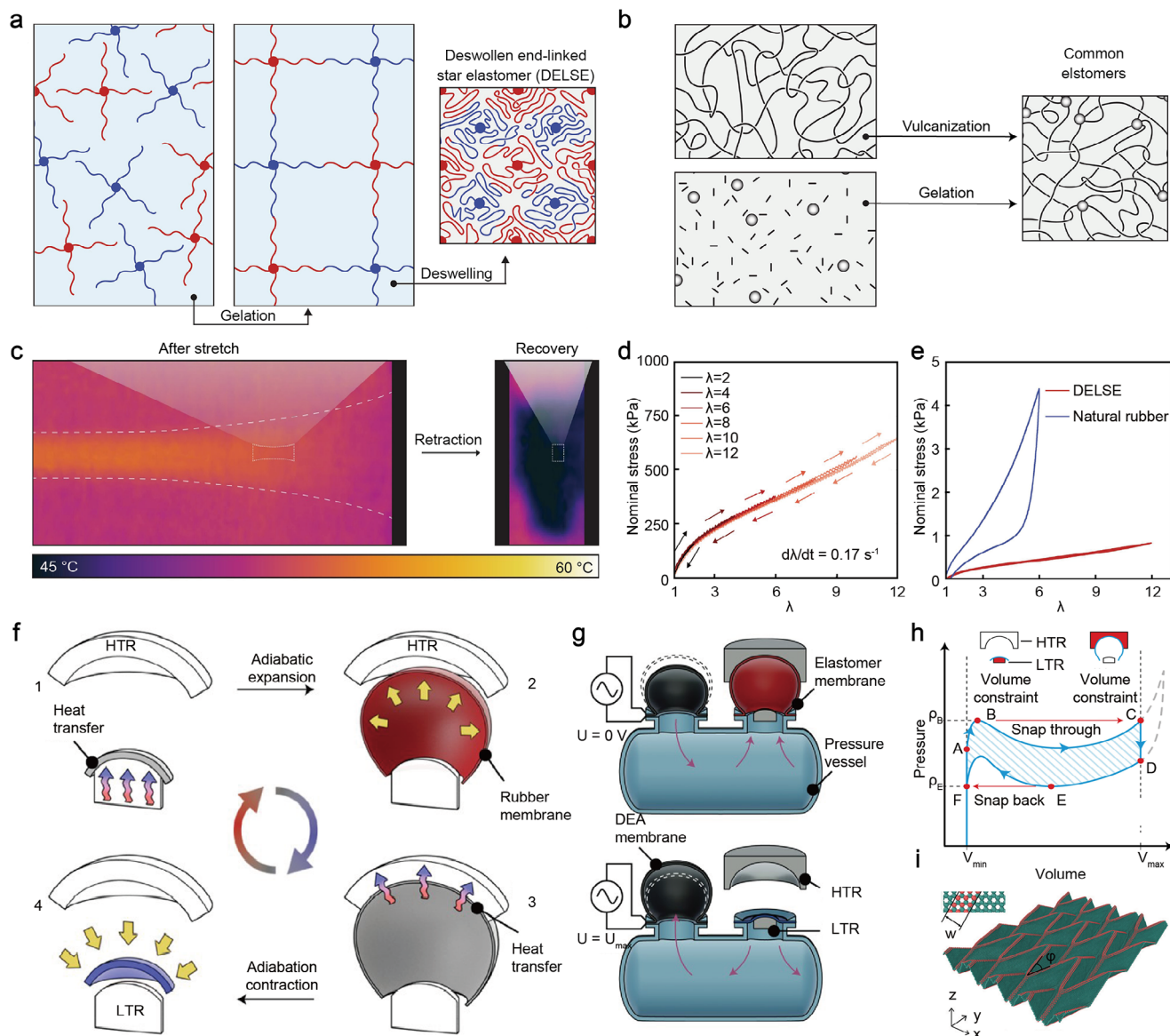


Figure 2. Elastocaloric effect in soft materials' systems. a) Schematic of homogeneous crosslinked polymers (DELSE) optimized for the elastocaloric effect. b) Schematics of the traditional random crosslinking process. c) Thermal images of the DELSE during retraction. d) Loading and unloading experiments, indicating negligible hysteresis at 60 °C. e) Mechanical performance comparisons between DELSE and natural rubber (NR). Reproduced with permission.^[28] Copyright 2023, American Association for the Advancement of Science. f) Utilizing the giant elastocaloric effect in a heat pump, combining it with a heat target (HTR) and a cooling target (LTR). g) Schematic illustration of the dielectric elastomer actuators (DEA)-actuated thermoregulation design and functional principle. h) Pressure–volume diagram of one actuation cycle. Reproduced with permission.^[33] Copyright 2021, Springer Nature. i) Schematic of utilization of origami metamaterials to enhance the elastocaloric effect. Reproduced with permission.^[34] Copyright 2024, ACS Publications.

to the cold side at a constant pressure (P_1), further lowering the system temperature to facilitate heat transfer from the cold side to the warm side.^[9,10,37]

Phase transitions in matter can be categorized as first-order (primary) and second-order (secondary) transitions. A first-order phase transition is characterized by a discontinuity in the system's free energy, such as Gibbs free energy, at the transition point. This phase transition is accompanied by the release or absorption of latent heat, as two distinct equilibrium phases coexist simultaneously. In crystal structure science, a first-order phase

transition can manifest as an abrupt change in lattice parameters or a significant alteration in crystal structure.^[38]

In first-order phase transition materials, phase transitions are typically accompanied by volume changes due to internal structural changes. For instance, a transition from a paramagnetic to a ferromagnetic state may cause a change in crystal structure, and this structural change triggers an abrupt volume change in the material.

Volume changes are generally closely related to variations in temperature and pressure. When the external pressure (Δp)

changes, especially near the phase transition temperature, the volume of the first-order phase transition material also undergoes significant changes. There is a strong relationship between the entropy change (ΔS) and the volume change (ΔV) during a first-order phase transition, which can be expressed by the following basic thermodynamic equation:

$$\Delta S = \int \frac{\Delta V}{T} dp \quad (2)$$

where ΔS is the entropy change that occurs in the material during the phase transition, ΔV is the change in volume of the material during the phase transition, and p is the pressure. This describes the relationship between entropy change and volume change when pressure changes are applied. In a first-order phase transition material, a change in pressure not only causes a significant change in volume but also affects the temperature through the entropy change. The temperature response becomes especially pronounced as the phase transition temperature is approached.

In contrast, a secondary phase transition is characterized by the continuity of the system's free energy and its derivatives at the transition point. Unlike first-order transitions, secondary phase transitions do not involve the release or absorption of latent heat, and only one equilibrium phase exists at the transition point. In the context of crystal structure science, a secondary phase transition is observed as a continuous change in lattice parameters, which may involve alterations in crystal symmetry without significant structural remodeling.^[39–42]

In certain magnetic materials, variations in hydrostatic pressure can induce changes in magnetic properties, often accompanied by structural crystallographic transitions or significant volume discontinuities. These factors can contribute to hysteresis in the BCE. Based on their microstructure, barocaloric materials can be categorized into several types, including plastic crystals, SMAs, ferroelastic materials, hybrid organic–inorganic chalcogenides, ferroelectric materials, molecular crystals, and *n*-alkanes.

Plastic crystals represent a promising next generation of barocaloric materials, showcasing significant entropic changes even at relatively low pressures. This unique behavior can be attributed to their highly disordered structure, which allows for large compressibility and unconventional lattice dynamics. These materials, often referred to as “oriented disordered crystals”, exhibit significant changes in entropy. This property makes them promising candidates for advanced thermoregulation applications. For example, the entropy change of the plastic crystal neopentyl glycol (NPG) near room temperature is about 389 J kg^{−1} K^{−1}. This value is ten times greater than that observed in currently known heat-generating materials (Figure 3a,b).^[36] The substantial entropy change observed in plastic crystals highlights their potential as soft systems, particularly in the context of bioelectronics and environmentally friendly thermoregulation technologies. Their adaptability and significant entropic changes position plastic crystals as promising candidates for efficient cooling solutions, underscoring their importance in the development of innovative and sustainable thermoregulation approaches for bioelectronic devices.

To achieve clean and sustainable energy at large scale and room temperature, Qian et al.^[43] designed a neopentyl glycol-based re-

frigeration cycle that utilizes its BCE. They proposed two potential schemes: a reverse Stirling cooling cycle and a reverse Brayton cooling cycle. The reverse Stirling cycle comprises two isobaric and two isothermal processes. During the phase from t_4 to t_1' , the heat source is cooled by harnessing the latent heat released during the phase transition of neopentyl glycol from a monoclinic to a cubic phase (CP) under high pressure (Figure 3c). The reverse Brayton cycle, in contrast, consists of two isobaric and two adiabatic processes. In the phases from t_1 to t_2 , the phase transition of neopentyl glycol from the monoclinic phase to the CP at low pressure is utilized to cool the heat source to a temperature lower than that of the source itself by adiabatically releasing pressure (Figure 3d). To validate these theoretical models, the research team designed and built a prototype for pressure card measurement. Through a cyclic pressurization and depressurization process, they varied the pressure from ambient conditions to 231 MPa at a temperature of 325 K, allowing them to observe the material's BCE. Specifically, they recorded an adiabatic 10 K pressurization ramp-up and a −16 K pressurization ramp-down in each of the 10 “pressurization–release” cycles, demonstrating that the BCE is both reversible and stable (Figure 3e–h).

Inspired by the enormous BCE found in plastic-crystalline materials, researchers have proposed the concept of a reverse BCE. This involves reverse barocaloric materials that release heat when pressurized, as opposed to conventional barocaloric materials. Zhang et al.^[44] introduced high reverse barocaloric batteries based on ammonium thiocyanate (NH₄SCN), which realizes the reverse barocaloric effect through a pressure-induced phase transition from an ordered to a disordered state (Figure 3i). Under pressure, NH₄SCN undergoes a continuous phase transition from a monoclinic to an orthorhombic phase, and finally to a tetragonal phase (Figure 3j,k,l). In the monoclinic phase, ND₄⁺ and SCN[−] ions are ordered, particularly with SCN[−] ions being oriented in an antiparallel manner. In the orthorhombic phase, the D atoms of the ND₄⁺ ions become disordered, forming a simple cubic lattice structure. These phase transitions are accompanied by an abrupt contraction of the unit cell volume by about 5%, leading to a significant change in a specific volume of about $-3.8 \times 10^{-5} \text{ m}^3 \text{ kg}^{-1}$. This large change in specific volume is a typical feature of the inverse BCE. In experiments, NH₄SCN absorbed heat during pressurization and released heat during depressurization, with the latent heat of charging being comparable to the latent heat of discharging, demonstrating high efficiency in converting mechanical energy—~11 times that of a conventional thermal battery (Figure 3j). This study not only showcases the novel application of the reverse barocaloric effect but also highlights NH₄SCN's potential as a high-efficiency thermoelectric material, particularly in harnessing pressure changes for energy conversion and saving. Its unique properties make it a promising candidate for thermoregulation applications, contributing to sustainable energy solutions by enhancing energy efficiency and reducing environmental impact.

Natural rubber, a chain polymer formed from the organic compound polypentadiene, is a low-cost, environmentally friendly elastomeric material. It exhibits BCEs and shows significant temperature changes when subjected to pressure. As a naturally soft system, NR's flexibility and responsiveness make it an excellent candidate for barocaloric technology applications. In 1805, Gough^[45] discovered that rubber undergoes a heat-absorbing

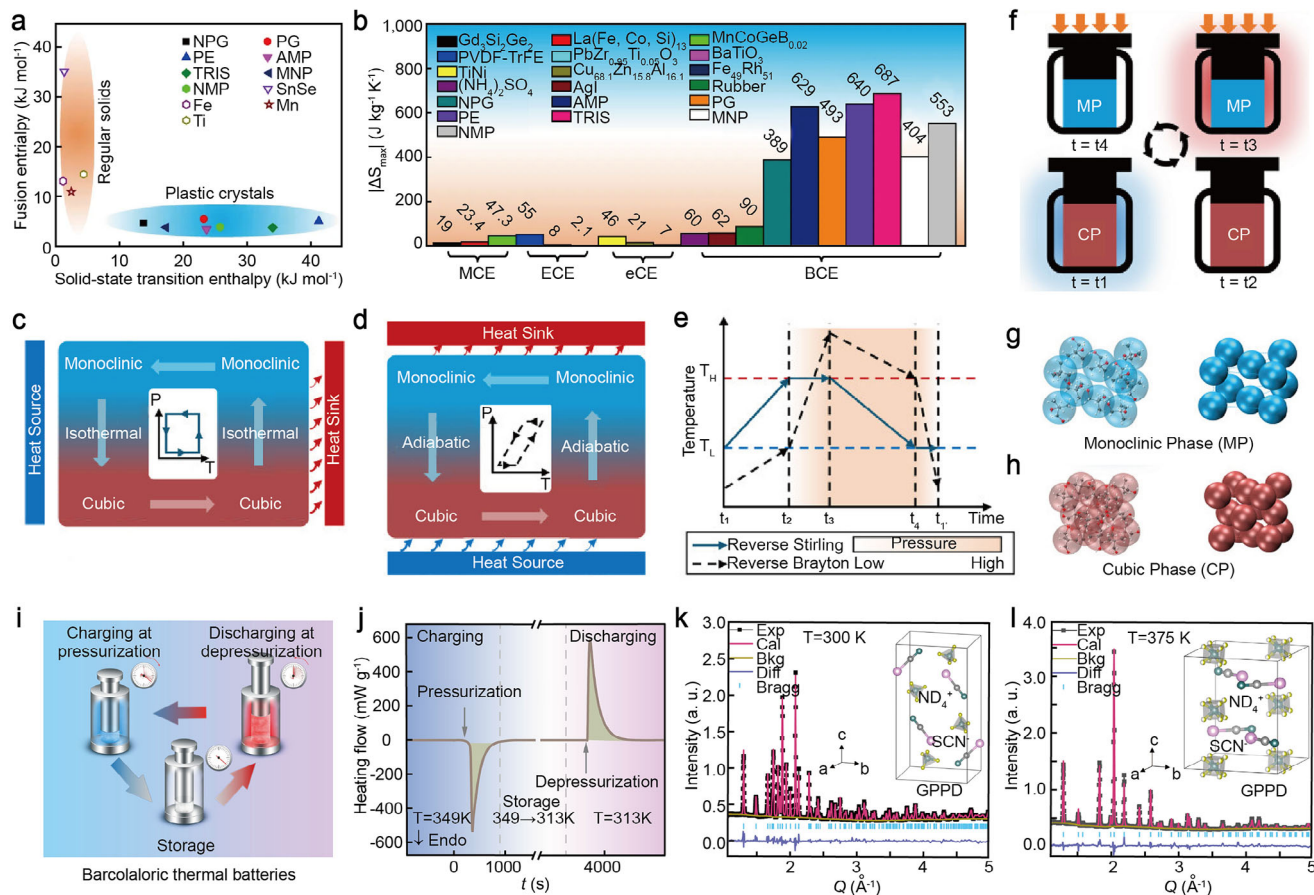


Figure 3. Barocaloric effect in soft materials' systems. a) Fusion enthalpy and solid-state transition enthalpy for typical regular solids and plastic crystals: neopentyl glycol (NPG), pentaglycerin (PG), pentaerythritol (PE), 2-amino-2-methyl-1,3-propanediol (AMP), tris(hydroxymethyl)aminomethane (TRIS), 2-methyl-2-nitro-1-propanol (MNP), 2-nitro-2-methyl-1,3-propanediol (NMP), tin selenide (SnSe), iron (Fe), manganese (Mn), titanium (Ti). b) Absolute values of maximum entropy changes, $|\Delta S_{\max}|$, for leading caloric materials. Reproduced with permission.^[36] Copyright 2019, Springer Nature. c) The reverse Stirling cooling cycle, consisting of two isobaric processes and two adiabatic processes that exchange heat with a heat source and a heat sink, respectively. d) The reverse Brayton cooling cycle, consisting of two isobaric and two adiabatic processes that exchange heat with a heat source and a heat sink, respectively. e) Temperature profiles for the reverse Stirling and reverse Brayton cooling cycles. The heat source temperature is T_L , and the heat sink temperature is T_H . f) Schematic of the pressure-driven barocaloric cooling cycle. Crystal structures of g) monoclinic phase (MP) and h) cubic phase (CP) NPG. Reproduced with permission.^[43] Copyright 2024, Cell Reports Physical Science. i) Schematic diagram for barocaloric thermal batteries including thermal charging at pressurization, storage, and thermal discharging at depressurization. j) Heat flow variations as a function of time for a barocaloric thermal battery process. k) Rietveld refinements of the neutron powder diffraction patterns of ND_4SCN at 300 K based on the $P2_1/c$ model and l) at 375 K based on the $Pbcm$ model (in the insets). Reproduced with permission.^[44] Copyright 2023, American Association for the Advancement of Science.

reaction when released after rapid stretching. Later, in 1942, Dart et al.^[46] observed a temperature change of about 12 K by rapid stretching. To explore NR's potential commercial thermoregulation, Bom et al.^[10] investigated its normalized temperature change and refrigerant capacity. Their results showed that the temperature change could reach up to 25 K under a pressure of about 390 MPa and a temperature of 314 K, with a strong dependence on the BCE related to NR's glass transition temperature.

SMA's typically undergo a martensitic transformation from a high-temperature, high-symmetry CP (austenite) to a low-temperature, low-symmetry, densely packed phase (martensite). This transformation includes alloys such as La-Fe-Si, Ni-Mn-Z (where Z can be Ga, Ti, In, Sn, or Sb), and Mn-Co-Ge.^[42,47-51] For example, Aznar et al.^[52] investigated the shape memory Heusler

alloy $\text{Ni}_{50}\text{Mn}_{31.5}\text{Ti}_{18.5}$, composed entirely of d-metal elements. By adjusting the composition, they eliminated the ferromagnetic order in this sample and achieved a maximum reversible isothermal entropy change of $35 \text{ J kg}^{-1} \text{ K}^{-1}$, demonstrating excellent barocaloric performance.

Typical ferroelectric materials, such as PbTiO_3 , $(\text{NH}_4)_2\text{SO}_4$, and BaTiO_3 , exhibit the BCE due to the coupling between lattice structures and electric dipole moments. Applying pressure can modulate the order of these electric dipole moments, thereby generating a barocaloric effect. For example, ammonium sulfate exists as a nonpolar crystal with an orthorhombic crystal structure at low temperatures. As the temperature approaches the ferroelectric phase transition temperature, ammonium sulfate undergoes a transition to a rhombohedral structure, accompanied by changes in polarization.

Perovskite materials, characterized by a basic structure of ABX_3 (where A is typically a large cation, B is a transition metal ion, and X is a small anion), demonstrate high responsiveness to changes in external pressure. In hybrid organic–inorganic perovskites, pressure changes can modulate both the electric dipole vector and the crystal structure, affecting the phase transition temperature and associate thermal effects.^[40,52–54]

These properties highlight the potential for mechanocaloric effects in soft materials, where the ability to manipulate pressure not only enhances energy conversion but also opens avenues for advanced thermoregulation solutions. By leveraging these mechanocaloric effects, BCE materials can play a crucial role in developing sustainable energy technologies.

3.3. Twistocaloric Effect in Soft Materials' Systems

Currently, thermoelectrics are the only commercially available solid-state thermoregulation technology. Vapor compression refrigeration typically has a Carnot efficiency of about 60%, whereas NiTi shape memory alloy-based tensile refrigeration can achieve a Carnot efficiency of $\approx 84\%$. To further enhance energy conversion efficiency and reduce costs, it is essential to advance the research and commercialization of mechanocaloric effect, particularly in soft systems.^[11,55] In 2019, Wang et al.^[56] proposed a torsional thermoregulation method based on twisting and coiling. Unlike elastocaloric effect, which involves uniaxial stress variation, and barocaloric effect, which involves hydrostatic pressure variation, torsional refrigeration originates from the twistocaloric effect. This effect results in temperature changes due to twisting in materials such as SMAs, polymers, and natural rubber. NR was selected as a typical twistocaloric material, and constant strains (100%, 250%, 300%, and 450%) were applied during the twisting process (Figure 4a). As shown in Figure 4b, under a 300% isometric strain, the average surface temperature changes of highly twisted, coiled, and partially supercoiled fibers were 3.3, 6.5, and 7.7 °C, respectively, while that of nontwisted fibers was 2.4 °C. Furthermore, by first releasing the twist and then applying a stretch, a greater maximum cooling effect of -16.4 °C and an average cooling effect of -14.5 °C were achieved. When using NR fibers composed of seven strands, each with a diameter of 2.2 mm, a maximum surface cooling temperature of -19.1 °C was attained.

The twistocaloric effect results of polyethylen demonstrated that the polyethylen braided fishing line was twisted at 6.5–7.3 rpm cm^{-1} under isobaric loads ranging from 37.1 to 74.2 MPa, with spring indices varying from 1.4 to 0.5. The maximum surface cooling temperature was -5.1 °C, while the average surface cooling temperature was -3.2 °C when a strain of 22.7% was released and the spring index was 0.8 (Figure 4c). The observed cooling effect is attributed to the entropy reduction caused by twisting, which leads to a partial transformation of the orthorhombic phase to the monoclinic phase in crystalline polyethylen fibers (Figure 4d,e).

While the temperature change is primarily induced by mechanical torsion, it still fundamentally involves the microstructural changes in the material under strain, similar to the entropy and volume changes in first-order phase change materials described by Equation (2). Specifically, the material's internal struc-

ture changes during torsion, leading to variations in both its volume and entropy, which, in turn, cause temperature changes.

According to the thermodynamic relation:

$$\Delta T = \frac{\Delta S}{C_p} \quad (3)$$

The temperature change resulting from entropy change depends on the material's specific heat capacity (C_p). During torsion, the entropy change of the material influences the temperature through this equation. For instance, at high strains, the material may undergo a larger entropy change, leading to a more pronounced temperature change.

For NiTi SMAs, reversible transformations between martensite and austenite occur during repeated cycles of twisting and untwisting. The twistocaloric efficiency remains stable, with a maximum surface cooling temperature of -17.0 °C achieved by isotropically untwisting a single NiTi filament at a torsional rate of 50 rpm at 0% strain. The cooling cycle of three strands of NiTi fibers is depicted in Figure 4f. Enhancing thermal insulation, enlarging the diameter of the channels, and increasing the rate of water flow can improve water cooling efficiency, resulting in a cooling effect of -7.7 °C (Figure 4f).

Poly(*p*-phenylbenzobisoxazole) (PBO) is an ideal material for mechanocaloric effect due to its ultrahigh thermal modulus and excellent thermal stability. However, because of the extreme rigidity of the PBO molecular chain, achieving better thermoregulation efficiency in elastocaloric refrigeration has been challenging. Feng et al.^[57] applied PBO fibers to torsional refrigeration to enhance cooling efficiency. They observed that increasing twist density led to higher surface temperature changes: the maximum heating temperature reached 7.2 K at 7 rpm cm^{-1} , with an average of 2.3 K. Similarly, the maximum cooling temperature change occurred at the same twist density, with peak values reaching -1.3 K and an average of -0.6 K. At a constant twist density, the temperature change of the fiber bundle increased with more twisting, although the maximum achievable twist density decreased. The molecular chains of pristine PBO fibers are aligned along the axial direction, and twisting enhances the crystallinity of the fibers. This helical arrangement reduces axial alignment, decreasing structural entropy and resulting in increased temperature. These properties highlight the potential of PBO as a soft material in bioelectronics, where efficient thermoregulation is critical. By leveraging the mechanocaloric effects in PBO, advancements can be made in developing technologies for sensitive bioelectronic devices, promoting both performance and sustainability.

Twisted fibers can induce temperature changes through torsional rotation or plying, while also possessing excellent mechanical stability, making them suitable for applications such as artificial muscles, wearable bioelectronics, thermoregulation, and biomedicine.^[58] For example, ions can be introduced into artificial muscles to control the dissociation of polymer chains and induce self-assembly through evaporation under external stress, resulting in high thermally driven supercontraction capabilities (Figure 4g,h).^[59] These unique properties not only inspire new designs for high-performance fiber materials and artificial muscles but also open up exciting possibilities for bioelectronics. By integrating twisted fibers into bioelectronic devices, we can

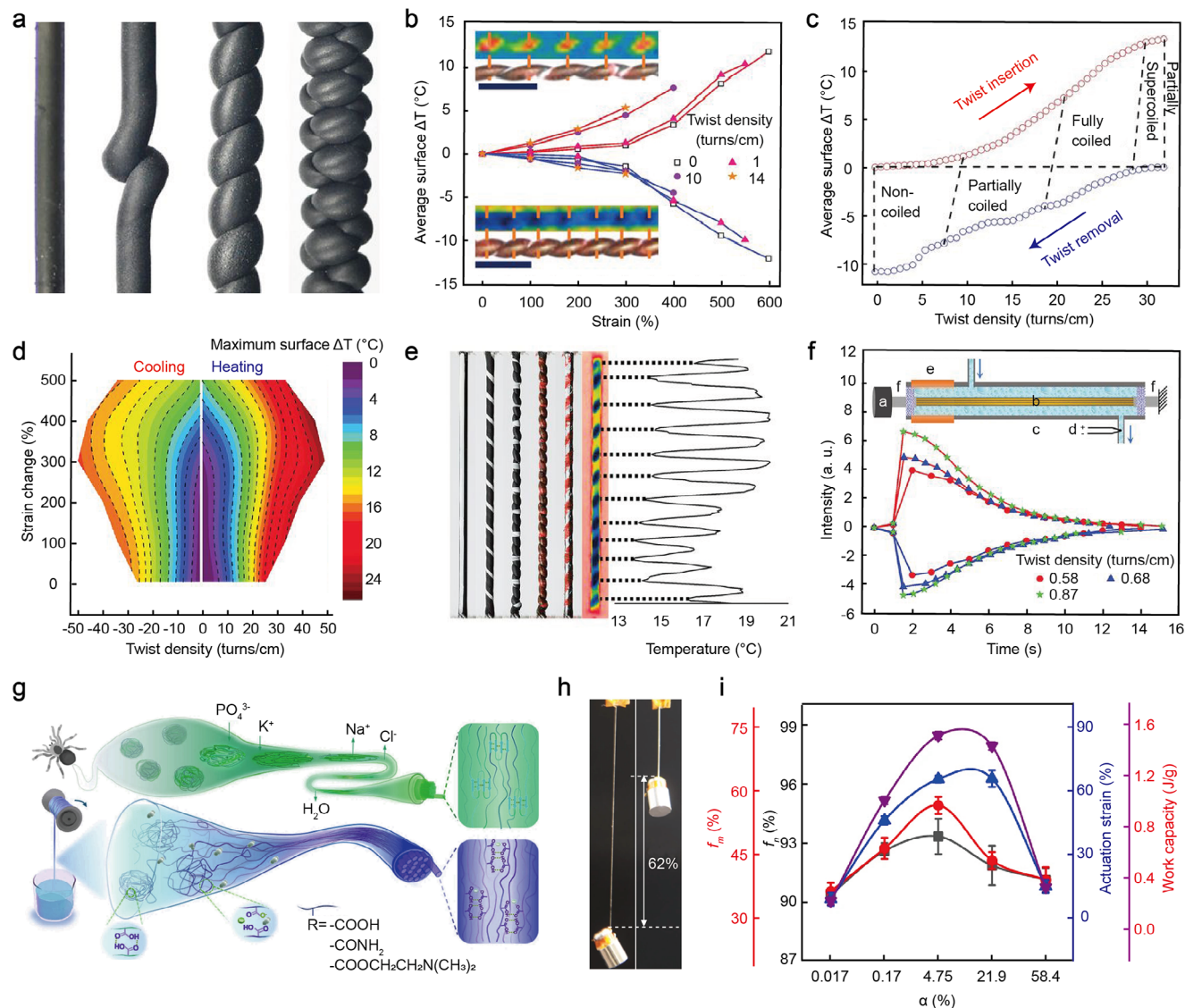


Figure 4. Twistocaloric effect in soft materials' systems. a) Photographs of twisted, partially coiled, fully coiled, and fully supercoiled 2.5 mm diameter NR fibers at 100% strain. b) Surface-average temperature changes versus strain for 0, 1, NR fibers with twists of 0, 1, 10, and 14 turns cm^{-1} (nontwisted, highly twisted, fully coiled, and partially supercoiled, respectively, in the nonstretched state). Scale bar: 0.5 mm. c) Surface-averaged temperature changes during equal-strength twisting and untwisting of NR fibers at 200% strain, measured continuously during an increasing and a decreasing twist scan. d) Maximum surface temperature change of NR fibers during continuous stretching and isometric twisting and during continuous isometric untwisting and stretch release. e) Photographs of an initially nontwisted, 3 cm long, 3 mm diameter NR fiber that was (from left to right) stretched to 100% and painted with a white line along its length, highly twisted, fully coiled, painted red on the coil's exterior, and then fully untwisted. f) Temperature change of effluent water as a function of time after isometric torsion insertion and removal of torsion from a triple-layered nickel–titanium wire. The device consists of a) motor, b) nitinol wire, c) polypropylene tubing with flowing water, d) thermocouple, e) rubber tubing, and f) epoxy resin for sealing the end of the tubing. Reproduced with permission.^[56] Copyright 2019, American Association for the Advancement of Science. g) Schematic of the spinning of spider silk and polyacrylic acid fiber (PAF α) artificial spider silk. h) Photographs of a 95 μm diameter PAF α 4.75% fiber before and after actuation (lifting a 2.0 g load). i) Dissociation (α value) corresponding to the actuation strain, workability, molecular chain orientation (f_m), and nanofiber orientation (f_n) of PAF α . Reproduced with permission.^[59] Copyright 2024, Springer Nature.

enhance their functionality and efficiency, paving the way for innovative solutions in soft robotics and responsive systems that require precise thermoregulation (Figure 4i).

It is important to emphasize that the three effects—elastocaloric, barocaloric, and twistocaloric—are fundamentally distinct in their mechanisms. Regarding the type of mechanical force, the elastocaloric effect occurs in solids subjected to uniaxial

forces such as stretching, compression, or tension. In contrast, the twistocaloric effect is induced by torsional stress, involving twisting, coiling, or rotational deformation. This type of stress generates force moments within the material, with significant effects being concentrated on the outer edges and minimal changes near the center, introducing a geometry-dependent behavior. However, the torsional forces also impose higher shear

Table 1. Physical properties for mechanocaloric materials.

Mechanocaloric materials	ΔT	Capability of cooling and heating	Δp [GPa]	Δs [J K ⁻¹ kg ⁻¹]	Refs.
Elastocaloric effect					
Natural rubber		Heating and cooling			[28–30]
Polystyrene- <i>b</i> -poly(ethylene-co-butylene)- <i>b</i> -polystyrene	500 K	Heating and cooling	0.26	326	[34]
Liquid crystalline elastomers	6 °C	Heating and cooling	0.001		[35]
Barocaloric effect					
Neopentyl glycol	14 K	Cooling	0.091	389	[36]
2-Amino-2-methyl-1,3-propanediol		Cooling		629	[36]
Ammonium thiocyanate	50 K	Heating and cooling	0.02	144	[44]
Natural rubber	25 K	Heating and cooling	0.39	59.0	[10]
La–Fe–Si	185–330 K	Cooling	0.1–0.32	5–17	[44,47–51]
Ni–Mn–Z (Z = Ga, Ti, In, Sn, or Sb)	12 K	Heating and cooling	0.4	85	[52]
Mn–Co–Ge	300 K	Cooling	0.05	23.5	[51]
PbTiO ₃	120 K	Cooling	0.1	1.6	[9,10,36]
BaTiO ₃	890 K	Cooling	0.26	2.7	[9,11,36]
(NH ₄) ₂ SO ₄	160 K	Cooling	0.03	80	[10,11,36]
Perovskite materials	5 K	Cooling	0.007	30.5	[40,53,54]
Spin-crossover materials	11 K	Cooling	0.001	78	[11]
Twistcaloric effect					
NiTi	14 K	Cooling		8.31	[55]
Natural rubber	19.1 °C	Cooling			[56]
Polyethylene	5.1 °C	Cooling	0.074		[56]
Poly(<i>p</i> -phenylbenzobisoxazole)	7.2 K	Heating and cooling	0.092		[57]

stress, leading to increased material fatigue. As a result, brittle or low-ductility materials are unsuitable for use in twistcaloric applications. To provide a clearer understanding of the mechanical forces involved and their impact on material properties, **Table 1** summarized the physical properties of various mechanocaloric materials.

4. Applications of Soft Mechanocaloric Materials

4.1. Sensing

The mechanocaloric effect, which connects mechanical energy with thermal energy, offers a unique approach to sensing small mechanical deformations. In recent years, there have been significant advancements in pressure sensors, such as piezoelectric sensors,^[60,61] triboelectric sensors,^[62,63] and magnetoelastic sensors.^[11,64] However, piezoelectric sensors predominantly rely on rigid materials, while triboelectric sensors depend on surface interactions and contact electrification, limiting their efficacy in detecting static mechanical stress. Although magnetoelastic materials can generate some heat due to the central area in the magnetic hysteresis loop, they are less efficient at converting mechanical energy into heat compared to mechanocaloric materials, which can directly convert mechanical energy into temperature changes.

Consequently, the mechanocaloric effect has broad applications in areas where temperature response is desired. For instance, elastic thermoelectric aerogels can monitor temperature changes and act as intelligent fire-warning systems. The applied pressure affects the structural integrity of the aerogels, altering

their heat generation efficiency. Enhanced aerogels, with their improved thermal properties, can serve as highly effective thermal insulation, protecting building structures from heat damage in extreme temperature environments.^[65] Temperature changes can also be detected by temperature sensors or captured by the thermoelectric effect,^[66,67] enhancing detection sensitivity and efficiently utilizing low-grade heat energy.^[68]

In addition, the mechanocaloric effect shows great potential in the field of bioelectronics. For example, sensors based on the mechanical thermoelectric effect can be used for real-time monitoring of human body temperature or other biological signals, and these sensors are not only highly sensitive, but also capable of providing noninvasive, wearable temperature control solutions in biomedical devices.

4.2. Therapeutics

Another promising application is personalized healthcare, offering comfort and health benefits by tailoring temperature settings to individual preferences.^[69] This can be achieved through either internal (active) or external (passive) thermoregulation. Internal temperature control uses therapeutic agents to adjust the body's physiological mechanisms, inducing heat generation.^[70] However, excessive reliance on internal regulation may lead to hyperthermia or hypothermia. Conversely, external temperature regulation employs wearable smart textiles and implantable devices to modulate temperature by absorbing or releasing heat, providing shade, controlling sweat evaporation, or converting other energy sources (such as mechanical energy) into heat.^[71] On the other

hand, the heat generated from the mechanocaloric effect can also be harnessed for thermal therapy or controlled drug release in cancer treatment.

The potential applications of bioelectronics in this field are vast.^[27,72] For example, wearable bioelectronic devices can integrate the mechanical thermal effect technology to achieve real-time temperature monitoring and regulation. These devices not only provide a comfortable temperature control experience but also provide real-time feedback on the user's physiological body temperature information, further promoting the development of personalized healthcare. On the other hand, the heat generated by the mechanothermal effect can also be used for controlled release of drugs in radiotherapy or cancer treatment, which provides new application prospects in the field of bioelectronics.

Given the high cooling performance of mechanocaloric devices compared to other solid-state cooling effects, such as magnetocaloric devices,^[73] mechanocaloric devices hold significant potential in the field of implantable devices. Excess heat generation is a critical issue in implantable brain-computer interfaces (BCIs), especially with the high integration and density of chips.^[74,75] Some BCI devices can reach temperatures as high as 330 K, well above the safe temperature limit for human brains (311 K),^[76] leading to hyperthermia and potential permanent structural damage. Implementing mechanocaloric systems in BCIs can ensure the long-term safety of these devices.

When comparing magnetocaloric and mechanocaloric effects, both adhere to the Clausius–Clapeyron equation and convert high-order energy to low-order energy (heat). In magnetocaloric materials, applying and removing magnets can induce temperature changes for cooling purposes, while in some cases, an alternating magnetic field can increase the overall temperature of the material.^[77,78] In contrast, mechanocaloric materials can achieve both heating and cooling by controlling stretching and releasing processes, making them versatile for various applications. In particular, bioelectronics shows great potential as one of the key application areas. For example, wearable devices based on the mechanical cooling effect are able to realize precise temperature control without relying on conventional power sources, thus providing a more efficient and long-lasting energy management solution for bioelectronic devices. These devices can not only be used for human temperature regulation, but can also be embedded into medical devices to achieve temperature control and drug release functions, thus promoting the development of personalized treatment and health monitoring. Innovative applications in the field of bioelectronics will revolutionize healthcare, health management, and disease prevention in the future.

4.3. Thermoregulation

Mechanocaloric systems utilize a variety of mechanical stimuli (stretching, pressure changes, and torsion) to induce temperature changes, providing precise thermoregulation. These technologies typically exhibit higher energy efficiency in the energy conversion process compared to traditional gas compression refrigeration systems. These advanced mechanocaloric systems offer precise temperature control, making them ideal for temperature-critical applications such as laboratory equipment and high-end electronics. Their applications in thermoregulation

include high-efficiency cooling equipment, energy recovery, automotive cooling systems, and intelligent buildings. Overall, these technologies not only enhance energy efficiency but also contribute to environmental protection.

The elastocaloric effect of NR was discovered over 160 years ago. However, the structural entropy change in NR polymers is limited by the uniformity of molecular chain length. Zhang et al.^[79] demonstrated that polystyrene–ethylene-*co*-butylene-*b*-styrene (SEBS) TPEs, with uniform molecular chain lengths, exhibit reversible conformational changes (Figure 5a–c). As shown in Figure 5a,b, the temperature change of a single elastocaloric cycle of SEBS, measured by infrared, shows a significant increase in the surface temperature of the TPEs from ambient temperature (299.0 K) during adiabatic stretching to 313.5 K (600% strain). During the stretch–recovery cycle, the shorter molecular chains in the TPE network are initially straightened, inhibiting further stretching of the longer molecular chains and thus limiting some conformational transitions. To address the high strain characteristics of rubber, a rotary motion cooling device was designed (Figure 5d). During the cooling process, the change in outlet temperature increased from 0.1 to 1.1 K as the strain amplitude increased from 100% to 600%. This study provides a strategy to enhance the elastocaloric effect, effectively releasing the cooling energy of polymer elastomers. This technology can be extended to soft solid-state cooling devices, creating new market opportunities and commercial value, while also offering potential applications in healthcare, such as wearable therapeutic cooling systems.

Mechanocaloric effects have significant potential in thermoregulation, particularly in bioelectronics, where precise local thermoregulation is crucial. However, in addition to polymer elastomers, soft SMAs have shown superior performance in solid-state cooling. Soft SMAs not only achieve higher cooling efficiencies during mechanical deformation, but their material properties also offer advantages in providing precise temperature control.^[52,80–82]

Ni–Mn–Ti and Ni–Ti alloys, recognized for their significant adiabatic temperature changes, are ideal materials for metal filaments in microcooling systems. To achieve high cooling power and a broad temperature range, Qian et al.^[14] designed an elastocaloric cooling system that utilizes four sets of tube flowing, axially loaded elastocaloric work mass bundles for multimode elastocaloric effect. This system achieves cooling by switching the flow paths of the heat transfer fluid network, enabling both single-stage and active heat return circulation (Figure 5e). As shown in Figure 5f, through multimode operation, the chiller achieves a maximum cooling temperature difference of 22.5 K and a cooling capacity of 260 W. In comparison, the single-stage cycle achieves only an 8 K cooling temperature difference, and the active reheat cycle achieves a cooling capacity of less than 30 W. This demonstrates the significant performance improvement achieved by the multimode elastocaloric chiller. The system maintains efficient operation across a broader range of conditions and optimizes the heat capacity ratio of the solid phase to the liquid phase in the tubular elastocaloric mass by adjusting its structural parameters. This advancement further promotes the commercialization of elastocaloric effect and other solid-state phase changes in cooling technologies.

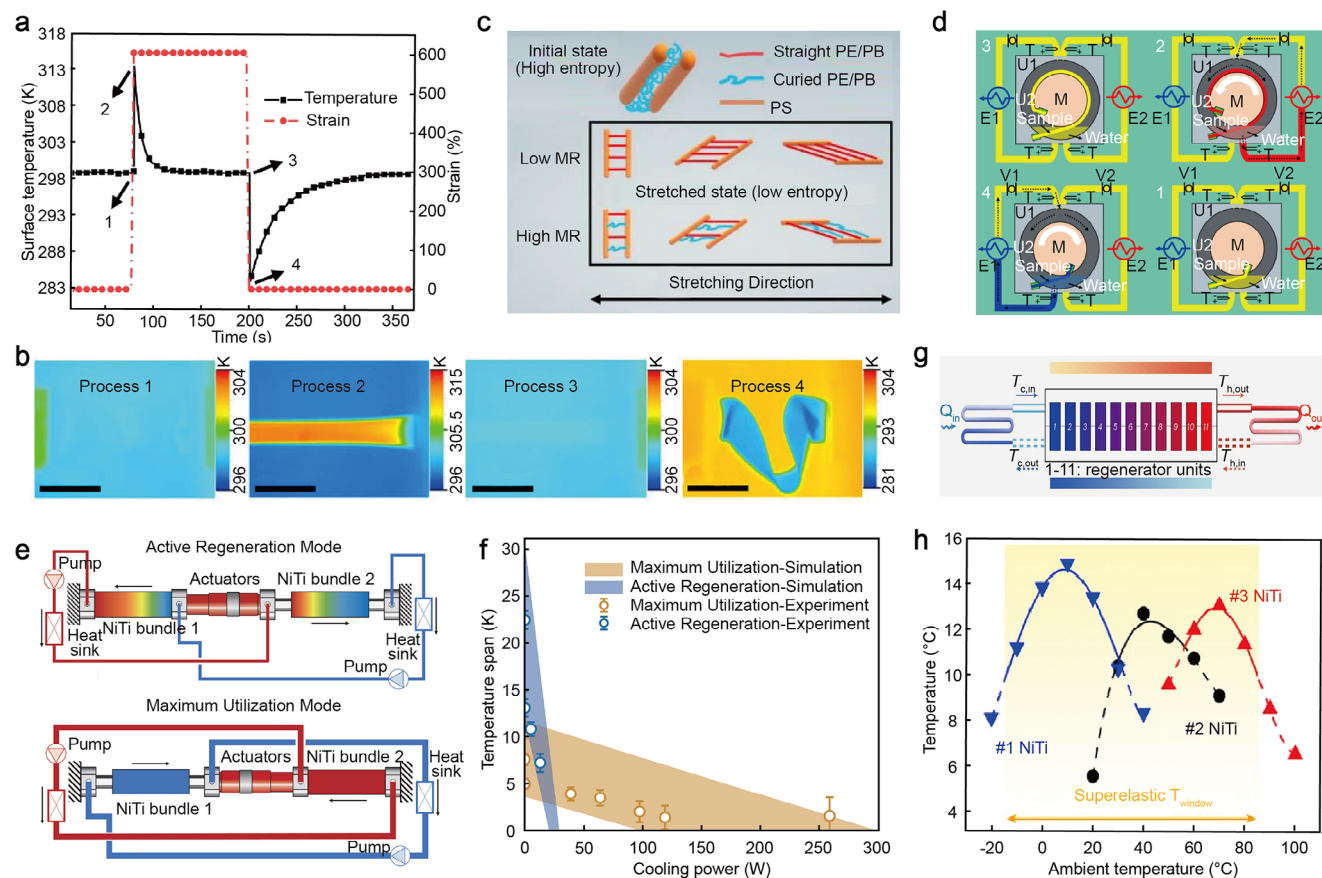


Figure 5. Showcasing of soft mechanocaloric materials for energy and healthcare. a) Typical strain evolution and resulting temperature changes in thermoplastic elastomers (TPEs) with the narrowest molecular weight distribution (TPE-1) during a single cycle of enormous elastocaloric effects (E-ECs). b) Infrared thermal images of the different processes recorded using an infrared thermal imager. c) Schematic diagram of PE/ poly(ethylene-co-butylene) (PB) conformational evolution during the stretching process of TPEs with different molecular weight distribution ranges (MRs). d) Schematic diagram of the rotary motion cooling device. These advancements in elastocaloric materials highlight their potential for highly efficient and sustainable thermoregulation, offering new pathways for next-generation cooling technologies and innovative healthcare applications. Reproduced with permission.^[79] Copyright 2022, Springer Nature. e) System design schematic and principle of operation of a multimode elastocaloric system. f) Temperature span versus cooling power for active regenerative mode (blue) and maximum utilization mode (orange) of a multimodal elastocaloric system. Reproduced with permission.^[14] Copyright 2023, American Association for the Advancement of Science. g) Schematic diagram of active regeneration in a multistage material cascade elastomeric regenerator. h) Variation of the adiabatic temperature changes of the #1, #2, and #3 NiTi SMAs with ambient temperature. Reproduced with permission.^[37] Copyright 2024, Springer Nature.

To further enhance the temperature difference in existing elastocaloric devices, Zhou et al.^[37] constructed a multimaterial cascade elastocaloric device using the reversible transformation of martensite and austenite in NiTi at three different temperatures. As shown in Figure 5g, the heat accumulator contains 11 multicell cross-sectional cascade tubular units made of NiTi with the largest specific heat transfer area ($12.5 \text{ cm}^2 \text{ g}^{-1}$). Each NiTi cell is 50 mm long, with ceramic loading heads being used to transfer forces between cells and to provide the heat exchange fluid, transferring heat from the low-temperature source to the high-temperature radiator. This multimaterial cascade structure achieves a superelastic temperature window of more than 100 °C for elastocaloric (ambient temperatures from -15 to 86 °C) with adiabatic temperature variations of more than 10 K (Figure 5h).

Soft mechanocaloric thermoregulation devices possess a wide array of applications in thermoregulation, including high-efficiency cooling, energy recovery, and automotive cooling. As

these technologies continue to be optimized, they will offer more market opportunities and environmental benefits, paving the way for broader commercialization.

5. Summary and Prospect

Mechanocaloric devices efficiently manipulate thermal energy, contributing significantly to thermoregulation through tailored heating and cooling. To further improve thermal management efficiency, promote environmental protection, and meet the needs of wearable electronics fields, it is critical to advance the development and commercialization of solid-state cooling technologies. Just as magnetocaloric technology research surged in the 1990s, mechanocaloric effect is poised to drive future innovations in thermal management. Advances in this field can provide more efficient and lightweight cooling solutions, enhancing the

performance and comfort of devices and extending the lifespan of soft equipment.

In this review, we have explored various aspects of the principles, classification, and applications of mechanocaloric effect-based thermoregulation technology, particularly in soft systems. This technology holds significant promise for several reasons. Compared to traditional refrigeration or heating systems, mechanocaloric effect can induce temperature changes directly through mechanical force, reducing the need for external energy. By optimizing the design of specific materials, the actual efficiency of the mechanocaloric effect can be very high. For example, ferromagnetic materials such as gadolinium-based alloys (Gd-based alloys) exhibit significant thermal effects during phase transitions and can approach the theoretical efficiency of the Carnot cycle.^[48,52,73,83]

Moreover, mechanocaloric technology is a green energy technology, significantly reducing environmental burdens and contributing to sustainable development. Additionally, it enables the design of miniaturized and compact systems based on materials such as metal wires, soft polymer fibers, and elastic films, which are especially advantageous for portable or miniature devices.^[37,84]

As global warming and the greenhouse effect intensify, there is a growing push to reduce greenhouse gas emissions to combat climate change. Amendments to the Paris Agreement and the Montreal Protocol encourage the adoption of thermoregulation solutions with low global warming potential, phasing out Hydrofluorocarbon (HFC)poly(ethylene-co-butylene)-based gas compression refrigeration technology.^[36,52,85,86]

Mechanocaloric effect based on soft systems has the potential to revolutionize the current field. In the meanwhile, electronic devices, sensors, and high-performance computers in high-tech field (such as aerospace missions) often require efficient cooling systems to maintain optimal operating temperatures. The mechanocaloric effect offers an efficient cooling method for improved thermoregulation. Specifically, solid-state cooling systems can be designed to be compact, portable, simple, and robust, making them well suited to withstand vibrations and shocks.^[87] This resilience reduces the risk of malfunctions and minimizes maintenance requirements.

There is a growing demand for smaller thermoregulation systems that can be integrated into more electronic devices to effectively manage waste heat, reduce power consumption, and meet requirements such as noise-free and wide-range temperature regulation. For example, blood analyzers and centrifuges are widely used in personalized healthcare, rehabilitation, and therapy.^[88–90] The biomedical reagents used in these devices contain biochemically active components that benefit from low temperatures, which help slow chemical reactions and degradation, thereby extending the reagents' stability and shelf life. Ventilator air pumps are key components that deliver air or oxygen into a patient's airway, ensuring adequate oxygen supply. These pumps use condensation and humidity control to improve equipment longevity, enhance patient comfort, and prevent harmful microorganism growth.^[60,91] Given its advantages—such as high efficiency, environmental protection, miniaturization, reliability, low maintenance, precise temperature control, and broad applicability—mechanocaloric technology is well positioned to

expand the utilization of thermoregulation systems in biomedical equipment. This expansion offers substantial benefits to personalized healthcare, enhancing the performance and reliability of critical medical devices. Consequently, mechanocaloric technologies based on soft systems are expected to find wider applications in various fields (Figure 6). Their simpler, more reliable structure and ease of integration make them ideal for these applications.

To further promote the application of mechanocaloric technology and enhance its cooling efficiency, comprehensive optimization is needed in material development, system design, technology integration, environmental simulation, and commercialization strategies. For example, exploring and developing new ferromagnetic materials, and further improving Gd-based alloys and other high-efficiency magnetocaloric materials, can increase the efficiency of the mechanocaloric effect.^[49,87] Additionally, developing multifunctional materials and applying nanotechnology and additive manufacturing to the microstructure design of engineered materials can enhance the reliability, lightweight, mechanical strength, and durability of thermoregulation systems. Moreover, developing detailed business and industrial promotion plans, understanding industry trends, analyzing market demand, and participating in the development of industry standards and specifications are essential steps to advance mechanocaloric technologies.^[9,33,92] For instance, automotive air conditioners are used to regulate the temperature and humidity inside vehicles, providing a comfortable environment for passengers. Current automotive air conditioners are compression-based systems that generate noise during operation, affecting the quiet interior environment.^[93,94] As mechanocaloric technology continues to advance and mature, it is expected to play an increasingly pivotal role in the automotive industry. This technology has the potential to enhance the overall performance of automotive cooling systems, leading to a quieter, more efficient user experience.

Mechanocaloric technology presents a viable solution as a miniaturized, flexible, efficient, and reliable temperature control system for soft robots.^[94–97] Such cooling systems can efficiently meet the thermal management needs of soft robots while operating noiselessly, which is crucial in environments that require minimal noise, such as medical settings, where surgical or assistive robots must perform procedures quietly and efficiently. In high-precision manufacturing environments, such as semiconductor and optical component processing, noise-free operation is also essential to avoid interference with experimental results.^[96–100] Although the initial cost of developing mechanocaloric technology is high, the cost is expected to decrease as the technology matures and production scales up. Understanding the market demand for high-efficiency, environmentally friendly, and stable cooling systems, promoting the technology, analyzing market trends, and adjusting product strategies will be crucial. Furthermore, deepening collaboration with suppliers, manufacturers, and system integrators can facilitate the commercialization and practical application of this technology.

Although mechanocaloric effect technology shows significant potential in the field of thermoregulation, it still faces a series of challenges in realizing large-scale applications, particularly in the following areas.

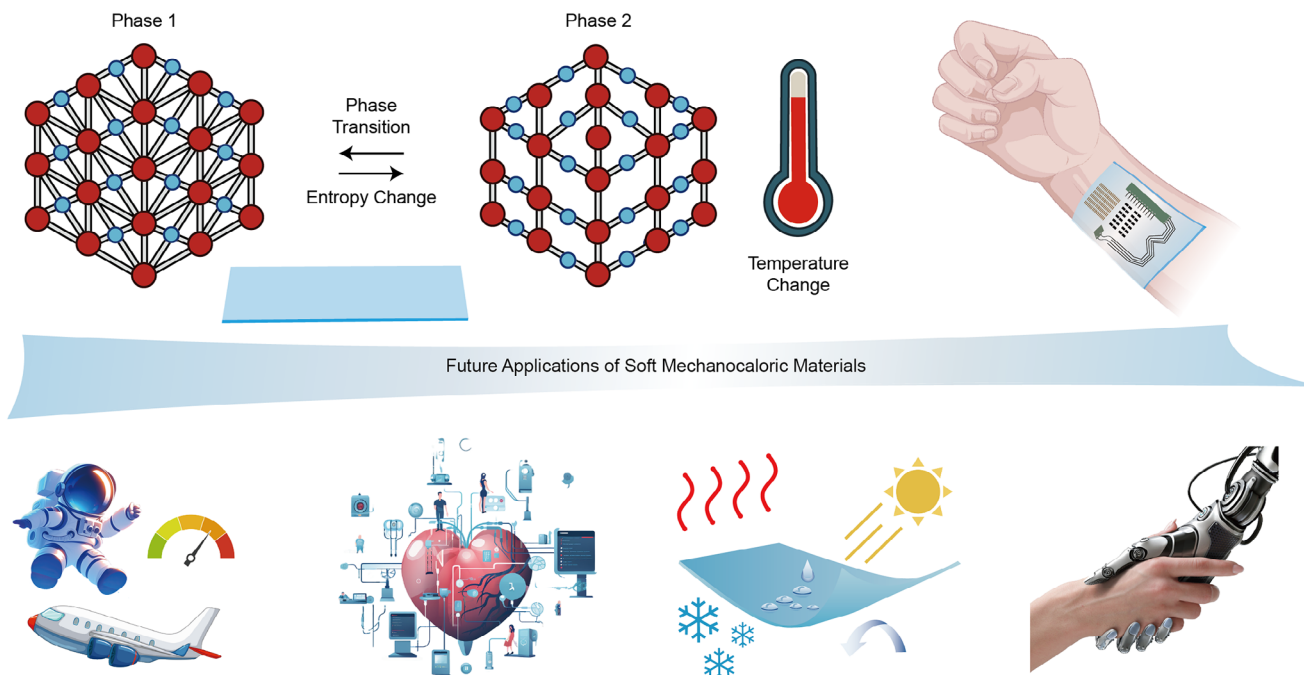


Figure 6. Mechanisms and future perspectives of soft mechanocaloric materials. The mechanocaloric effect offers an efficient cooling method that enhances thermoregulation. These systems can be designed to be compact, portable, and robust, allowing them to withstand vibrations and shocks, thereby reducing the risk of malfunctions and minimizing maintenance. The demand for smaller, highly integrated thermoregulation systems is growing, driven by the need to manage waste heat effectively, lower power consumption, and enable noise-free operation with broad thermal regulation. Applications span diverse fields, including aerospace, biomedical systems, engineered refrigeration materials, and soft robotics. Mechanocaloric systems provide flexible, efficient thermal management solutions, ensuring optimal performance and reliability in complex, dynamic environments.

5.1. Inadequate Refrigeration Efficiency

Current mechanocaloric technologies have yet to achieve the desired level of refrigeration efficiency, especially under high loads or during prolonged operation. While these technologies can create a certain temperature difference, their cooling effect remains weaker compared to traditional refrigeration technologies (such as compressor cooling, Peltier effect),^[101,102] particularly when large-scale cooling or rapid temperature changes are required. Conventional refrigeration methods still have a clear advantage in handling large amounts of heat, providing more stable and powerful cooling. In contrast, mechanocaloric effect technologies, especially those using soft materials (such as elastomers and polymers), need further improvement in energy efficiency and cooling performance. However, the inherent flexibility and deformability of soft materials provide significant advantages, offering better adaptability and comfort in more complex applications. Efficiency may be enhanced by the development of new materials such as high-entropy alloys and SMAs, which exhibit higher entropy changes, stronger mechanical strain responses, and lower thermal conductivity.^[103]

5.2. Miniaturization and Wearability

Mechanocaloric technologies hold great potential for miniaturization, particularly with soft materials, which allow for the de-

sign of lighter and more flexible devices. This makes them especially suitable for wearable devices. However, current devices are generally larger, and the complexity of designing the cooling units and materials makes them unsuitable for everyday wearable applications. Devices made from soft materials offer better adaptability and comfort than traditional cooling technologies, particularly in wearable applications where the materials can conform to the body's shape and provide a degree of elasticity. However, the rigidity and weight of materials remain key obstacles to their application. In addition to size and comfort, wearable devices must also withstand complex and dynamic environments. For instance, wearable devices worn on the human body must account for factors such as mechanical vibrations, body movements, and fluctuations in body temperature, all of which can influence the device's cooling performance.^[104] Furthermore, in industrial settings, these devices need to function effectively in environments with varying humidity, mechanical stress, and high temperatures. To tackle these challenges, advanced micromachining techniques and miniaturized thermoregulation designs can be utilized to reduce device size while preserving cooling efficiency. Additionally, employing flexible film materials and stretchable structures can help overcome the stiffness and discomfort often associated with traditional materials. These innovations will enable wearable devices to remain both functional and comfortable, even under demanding conditions like physical movement or industrial vibrations, ultimately enhancing the technology's flexibility, adaptability, and overall performance.

5.3. Stability and Durability

The stability and durability of mechanocaloric technologies in real-world environments remain insufficient, particularly with soft materials, where long-term mechanical strain (such as repeated twisting and stretching) can lead to fatigue and performance degradation.^[105–107] Compared to traditional compressor-based refrigeration systems, soft materials may lose some of their effectiveness after extended mechanical deformation, impacting the overall reliability of the device. While soft materials such as elastomers and polymers offer significant comfort advantages, they require further strengthening in terms of durability and stability, especially in applications involving frequent deformation or long-term use.^[64,108–112] The degradation of soft materials' performance can be mitigated through material optimization and surface treatments to improve their stability in harsh environments.

5.4. Scalability and Cost

Soft material-based mechanocaloric effect technology offers certain cost advantages over traditional compressor refrigeration methods. While traditional refrigeration relies on complex mechanical systems and energy-intensive refrigerants, soft material technology utilizes the thermoresponsive properties of the materials themselves, simplifying the manufacturing process and reducing energy consumption. However, the current soft material mechanocaloric technologies still face high production costs, particularly when developing new high-performance materials and efficient heat transfer systems. Despite the advantages of miniaturization and lightweight designs, soft materials still need to be optimized in terms of cost and production efficiency to enable large-scale production and application. Production costs can be reduced by optimizing material synthesis and improving manufacturing processes, with mass production further driving down unit costs.^[113,114]

In summary, the emergence of thermoregulation technology based on the mechanocaloric effect offers a new pathway in sensing, therapy, and thermoregulation. To enhance the effectiveness of thermoregulation technologies, further research is necessary to optimize cooling efficiency, reduce device size for improved wearability, and ensure stability under various conditions. Scalability is also crucial for broader applications in bioelectronics and soft materials.^[115–118] Establishing industry standards will help guide development and ensure consistency. As mechanocaloric advances and costs come down, it is set to become a go-to choice for thermoregulation, driving sustainable development and green technology forward.

Acknowledgements

X.F. and S.C. contributed equally to this work. The authors acknowledge the Henry Samueli School of Engineering & Applied Science and the Department of Bioengineering at the University of California, Los Angeles, for their startup support. J.C. acknowledged the Vernroy Makoto Watanabe Excellence in Research Award at the UCLA Samueli School of Engineering, the Office of Naval Research Young Investigator Award (Award ID. N00014-24-1-2065), National Institutes of Health Grant (Award ID.

R01 CA287326), National Science Foundation Grant (Award No. 2425858), the American Heart Association Innovative Project Award (Award ID: 231PA1054908), the American Heart Association Transformational Project Award (Award ID: 23TPA1141360), and the American Heart Association's Second Century Early Faculty Independence Award (Award ID: 23SCE-FIA1157587).

Conflict of Interest

The authors declare no conflict of interest.

Keywords

barocaloric effect, bioelectronics, elastocaloric effect, mechanocaloric effects, twistocaloric effect

Received: November 1, 2024

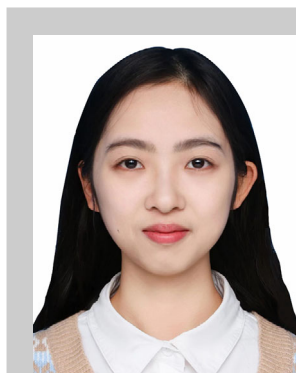
Revised: March 13, 2025

Published online:

- [1] S. Pu, J. Fu, Y. Liao, L. Ge, Y. Zhou, S. Zhang, S. Zhao, X. Liu, X. Hu, K. Liu, J. Chen, *Adv. Mater.* **2020**, *32*, 1907307.
- [2] S. Pu, Y. Liao, K. Chen, J. Fu, S. Zhang, L. Ge, G. Conta, S. Bouzarif, T. Cheng, X. Hu, K. Liu, J. Chen, *Nano Lett.* **2020**, *20*, 3791.
- [3] Q. Wang, C. R. Bowen, R. Lewis, J. Chen, W. Lei, H. Zhang, M. Y. Li, S. Jiang, *Nano Energy* **2019**, *60*, 144.
- [4] L. Liu, J. Chen, L. Liang, L. Deng, G. Chen, *Nano Energy* **2022**, *102*, 107678.
- [5] X. Moya, N. Mathur, *Science* **2020**, *370*, 797.
- [6] L. Cai, A. Y. Song, W. Li, P. C. Hsu, D. Lin, P. B. Catrysse, Y. Liu, Y. Peng, J. Chen, H. Wang, J. Xu, A. Yang, S. Fan, Y. Cui, *Adv. Mater.* **2018**, *30*, 1802152.
- [7] L. Cai, A. Y. Song, P. Wu, P. C. Hsu, Y. Peng, J. Chen, C. Liu, P. B. Catrysse, Y. Liu, A. Yang, C. Zhou, C. Zhou, S. Fan, Y. Cui, *Nat. Commun.* **2017**, *8*, 496.
- [8] Y. Peng, J. Chen, A. Y. Song, P. B. Catrysse, P. C. Hsu, L. Cai, B. Liu, Y. Zhu, G. Zhou, D. S. Wu, H. R. Lee, S. Fan, Y. Cui, *Nat. Sustainability* **2018**, *1*, 105.
- [9] L. Cirillo, A. Greco, C. Masselli, *Therm. Sci. Eng. Prog.* **2022**, *33*, 101380.
- [10] N. M. Bom, E. O. Usuda, L. S. Paixão, A. M. G. Carvalho, *ACS Macro Lett.* **2018**, *7*, 31.
- [11] H. L. Hou, S. X. Qian, I. Takeuchi, *Nat. Rev. Mater.* **2022**, *7*, 633.
- [12] H. Y. Qian, J. P. Guo, Z. Y. Wei, J. Liu, *Phys. Rev. Mater.* **2022**, *6*, 054401.
- [13] H. Hou, E. Simsek, T. Ma, N. S. Johnson, S. Qian, C. Cissé, D. Stasak, N. Al Hasan, L. Zhou, Y. Hwang, *Science* **2019**, *366*, 1116.
- [14] S. Qian, D. Catalini, J. Muehlbauer, B. Liu, H. Mevada, H. Hou, Y. Hwang, R. Radermacher, I. Takeuchi, *Science* **2023**, *380*, 722.
- [15] E. Bonnot, R. Romero, L. Manosa, E. Vives, A. Planes, *Phys. Rev. Lett.* **2008**, *100*, 125901.
- [16] J. Tušek, K. Engelbrecht, D. Eriksen, S. Dall'Olio, J. Tušek, N. Pryds, *Nat. Energy* **2016**, *1*, 16134.
- [17] L. Mañosa, A. Planes, *Adv. Mater.* **2017**, *29*, 1603607.
- [18] Y. Zhou, X. Zhao, J. Xu, Y. Fang, G. Chen, Y. Song, S. Li, J. Chen, *Nat. Mater.* **2021**, *20*, 1670.
- [19] G. Chen, X. Zhao, S. Andalib, J. Xu, Y. Zhou, T. Tat, K. Lin, J. Chen, *Matter* **2021**, *4*, 3725.
- [20] Y. Fang, X. Zhao, G. Chen, T. Tat, J. Chen, *Joule* **2021**, *5*, 752.
- [21] Y. Wu, E. Ertekin, H. Sehitoglu, *Acta Mater.* **2017**, *135*, 158.

- [22] Z. Ahcin, S. Dall'Olio, A. Zerovnik, U. Z. Baskovic, L. Porenta, P. Kabirifar, J. Cerar, S. Zupan, M. Brojan, J. Klemenc, J. Tusek, *Joule*. **2022**, *6*, 2338.
- [23] W. M. Awad, D. W. Davies, D. Kitagawa, J. M. Halabi, M. B. Al-Handawi, I. Tahir, F. Tong, G. Campillo-Alvarado, A. G. Shtukenberg, T. Alkhidir, Y. Hagiwara, M. Almehairbi, L. Lan, S. Hasebe, D. P. Karothu, S. Mohamed, H. Koshima, S. Kobatake, Y. Diao, R. Chandrasekar, H. Zhang, C. C. Sun, C. Bardeen, R. O. Al-Kaysi, B. Kahr, P. Naumov, *Chem. Soc. Rev.* **2023**, *52*, 3098.
- [24] X. Zhao, Y. Zhou, Y. Song, J. Xu, J. Li, T. Tat, G. Chen, S. Li, J. Chen, *Nat. Mater.* **2024**, *23*, 703.
- [25] X. Zhao, Y. Zhou, W. Kwak, A. Li, S. Wang, M. Dallenger, S. Chen, Y. Zhang, A. Lium, J. Chen, *Nat. Commun.* **2024**, *15*, 8492.
- [26] X. Zhao, Y. Zhou, A. Li, J. Xu, S. Karjagi, E. Hahm, L. Rulloda, J. Li, J. Hollister, P. Kavehpour, J. Chen, *Nat. Electron.* **2024**, *7*, 924.
- [27] X. Zhao, Y. Zhou, J. Xu, G. Chen, Y. Fang, T. Tat, X. Xiao, Y. Song, S. Li, J. Chen, *Nat. Commun.* **2021**, *12*, 6755.
- [28] C. M. Hartquist, S. Lin, J. H. Zhang, S. Wang, M. Rubinstein, X. Zhao, *Sci. Adv.* **2023**, *9*, adj0411.
- [29] C. Cazorla, *Appl. Phys. Rev.* **2019**, *6*, 041316.
- [30] B. F. Lu, J. Liu, *Sci. Bull.* **2015**, *60*, 1638.
- [31] K. J. Chua, S. K. Chou, W. M. Yang, *Appl. Energy*. **2010**, *87*, 3611.
- [32] G. Sachdeva, A. Jaiswar, P. Anuradha, V. Jain, *Int. J. Air-Cond. Refrig.* **2023**, *31*, 20.
- [33] F. Greibich, R. Schwödauer, G. Mao, D. Wirthl, M. Drack, R. Baumgartner, A. Kogler, J. Stadlbauer, S. Bauer, N. Arnold, *Nat. Energy*. **2021**, *6*, 260.
- [34] J. Cai, B. Yang, A. Akbarzadeh, *ACS Nano*. **2024**, *18*, 894.
- [35] J. A. Herman, J. D. Hoang, T. J. White, *Small*. **2024**, *20*, 2400786.
- [36] B. Li, Y. Kawakita, S. Ohira-Kawamura, T. Sugahara, H. Wang, J. Wang, Y. Chen, S. I. Kawaguchi, S. Kawaguchi, K. Ohara, K. Li, *Nature*. **2019**, *567*, 506.
- [37] G. Zhou, Z. Li, Q. Wang, Y. Zhu, P. Hua, S. Yao, Q. Sun, *Nat. Energy*. **2024**, *9*, 862.
- [38] Y. Ling, Y. Hu, H. Wang, B. Niu, J. Chen, R. Liu, Y. Yuan, G. Wang, D. Wu, M. Xu, Z. Han, J. Du, Q. Xu, *ACS Appl. Mater. Interfaces*. **2021**, *13*, 24285.
- [39] T. Lei, K. Engelbrecht, K. K. Nielsen, H. N. Bez, C. R. H. Bahl, *J. Phys. D: Appl. Phys.* **2016**, *49*, 345001.
- [40] J. M. Bermúdez-García, M. Sánchez-Andújar, S. Castro-García, J. López-Beceiro, R. Artiaga, M. A. Señaris-Rodríguez, *Nat. Commun.* **2017**, *8*, 15715.
- [41] Z. Zhao, G. Chen, X. Liu, L. Shao, Y. Xu, X. Zhang, Y. Li, Z. Yan, T. Zou, *Energy Fuels*. **2023**, *37*, 6348.
- [42] X. Moya, L. E. Hueso, F. Maccherozzi, A. I. Tovstolytkin, D. I. Podyalovskii, C. Ducati, L. C. Phillips, M. Ghidini, O. Hovorka, A. Berger, M. E. Vickers, E. Defay, S. S. Dhesi, N. D. Mathur, *Nat. Mater.* **2013**, *12*, 52.
- [43] K. Qian, S. Lin, Z. Zhang, B. Li, Y. Peng, Y. Li, C. Zhao, *Cell Rep. Phys. Sci.* **2024**, *5*, 101981.
- [44] Z. Zhang, K. Li, S. C. Lin, R. Q. Song, D. H. Yu, Y. D. Wang, J. F. Wang, S. Kawaguchi, Z. Zhang, C. Y. Yu, X. D. Li, J. Chen, L. H. He, R. Mole, B. Yuan, Q. Y. Ren, K. Qian, Z. L. Cai, J. G. Yu, M. C. Wang, C. Y. Zhao, X. Tong, Z. D. Zhang, B. Li, *Sci. Adv.* **2023**, *9*, add0374.
- [45] M. Gough, *Mem. Lit. Phil. Soc. Manchester* **1805**, *1*, 288.
- [46] S. L. Dart, R. L. Anthony, E. Guth, *Ind. Eng. Chem.* **1942**, *34*, 1340.
- [47] A. A. P. Lloveras, M. Barrio, Ph. Negrier, C. Popescu, A. Planes, L. Mañosa, E. Stern-Taulats, A. Avramenko, N. D. Mathur, X. Moya, J. Li Tamarit, *Nat. Commun.* **2018**, *10*, 1803.
- [48] Z. Q. Zhao, M. M. Xue, H. Qiu, W. L. Guo, Z. H. Zhang, *Cell Rep. Phys. Sci.* **2022**, *3*, 100822.
- [49] V. M. Andrade, N. B. Barroca, A. L. Pires, J. H. Belo, A. M. Pereira, K. R. Pirota, J. P. Araújo, *Mater. Design*. **2020**, *186*, 108354.
- [50] A. Kitanovski, *Adv. Energy Mater.* **2020**, *10*, 1903741.
- [51] N. R. Ram, M. Prakash, U. Naresh, N. S. Kumar, T. S. Sarmash, T. Subbarao, R. J. Kumar, G. R. Kumar, K. C. B. Naidu, *J. Supercond. Novel Magn.* **2018**, *31*, 1971.
- [52] A. Aznar, A. Gràcia-Condal, A. Planes, P. Lloveras, M. Barrio, J. L. Tamarit, W. Xiong, D. Cong, C. Popescu, L. Mañosa, *Phys. Rev. Mater.* **2019**, *3*, 044406.
- [53] D. Y. Kim, S. Kim, S. A. Lee, Y. E. Choi, W. J. Yoon, S. W. Kuo, C. H. Hsu, M. Huang, S. H. Lee, K. U. Jeong, *J. Phys. Chem. C*. **2014**, *118*, 6300.
- [54] T. P. Chen, J. X. Lin, C. C. Lin, C. Y. Lin, W. C. Ke, D. Y. Wang, H. S. Hsu, C. C. Chen, C. W. Chen, *ACS Appl. Mater. Interfaces*. **2021**, *13*, 10279.
- [55] G. V. Brown, *J. Appl. Phys.* **1976**, *47*, 3673.
- [56] R. Wang, S. Fang, Y. Xiao, E. Gao, N. Jiang, Y. Li, L. Mou, Y. Shen, W. Zhao, S. Li, A. F. Fonseca, D. S. Galvão, M. Chen, W. He, K. Yu, H. Lu, X. Wang, D. Qian, A. E. Aliev, N. Li, C. S. Haines, Z. Liu, J. Mu, Z. Wang, S. Yin, M. D. Lima, B. An, X. Zhou, Z. Liu, R. H. Baughman, *Science*. **2019**, *366*, 216.
- [57] D. Feng, Y. Xiao, G. Wang, G. Mei, W. Guo, K. Yu, S. Liu, W. Zhao, X. Zhou, Z. Liu, *Macromol. Rapid Commun.* **2023**, *44*, 2300318.
- [58] X. Leng, X. Hu, W. Zhao, B. An, X. Zhou, Z. Liu, *Adv. Intell. Syst.* **2021**, *3*, 2000185.
- [59] W. He, M. Wang, G. Mei, S. Liu, A. Khan, C. Li, D. Feng, Z. Su, L. Bao, G. Wang, E. Liu, Y. Zhu, J. Bai, M. Zhu, X. Zhou, Z. Liu, *Nat. Commun.* **2024**, *15*, 3485.
- [60] W. Deng, Y. Zhou, A. Libanori, G. Chen, W. Yang, J. Chen, *Chem. Soc. Rev.* **2022**, *51*, 3380.
- [61] Y. Su, C. Chen, H. Pan, Y. Yang, G. Chen, X. Zhao, W. Li, Q. Gong, G. Xie, Y. Zhou, *Adv. Funct. Mater.* **2021**, *31*, 2010962.
- [62] J. Lama, A. Yau, G. Chen, A. Sivakumar, X. Zhao, J. Chen, *J. Mater. Chem. A*. **2021**, *9*, 19149.
- [63] Y. Zou, V. Raveendran, J. Chen, *Nano Energy*. **2020**, *77*, 105303.
- [64] Y. Zhou, X. Zhao, J. Xu, G. Chen, T. Tat, J. Li, J. Chen, *Sci. Adv.* **2024**, *10*, adj8567.
- [65] H. Li, Z. Ding, Q. Zhou, J. Chen, Z. Liu, C. Du, L. Liang, G. Chen, *Nano-Micro. Lett.* **2024**, *16*, 151.
- [66] X. L. Shi, J. Zou, Z. G. Chen, *Chem. Rev.* **2020**, *120*, 7399.
- [67] J. Li, B. Xia, X. Xiao, Z. Huang, J. Yin, Y. Jiang, S. Wang, H. Gao, Q. Shi, Y. Xie, J. Chen, *ACS Nano*. **2023**, *17*, 19232.
- [68] X. Li, X. Xiao, C. Bai, M. Mayer, X. Cui, K. Lin, Y. Li, H. Zhang, J. Chen, *J. Mater. Chem. C*. **2022**, *10*, 13789.
- [69] Y. Fang, G. Chen, M. Bick, J. Chen, *Chem. Soc. Rev.* **2021**, *50*, 9357.
- [70] S. Chen, J. Wang, L. Sun, F. Xia, W. Li, L. Yuan, C. Liu, P. Li, C. Bao, M. Wang, G. Wang, J. Li, Y. Xie, W. Lu, *Biomaterials*. **2024**, *311*, 122687.
- [71] S. Chen, F. Manshahi, X. Fan, Z. Duan, X. Zhao, Y. Zhou, J. Chen, *Matter*. **2024**, *7*, 2632.
- [72] J. Yin, S. Wang, T. Tat, J. Chen, *Nat. Rev. Bioeng.* **2024**, *2*, 541.
- [73] H. Hou, P. Finkel, M. Staruch, J. Cui, I. Takeuchi, *Nat. Commun.* **2018**, *9*, 4075.
- [74] G. Lazzi, *IEEE Eng. Med. Biol. Mag.* **2005**, *24*, 75.
- [75] G. Kim, J. H. In, Y. Lee, H. Rhee, W. Park, H. Song, J. Park, J. B. Jeon, T. D. Brown, A. A. Talin, S. Kumar, K. M. Kim, *Nat. Mater.* **2024**, *23*, 1237.
- [76] H. Wang, B. Wang, K. P. Normoyle, K. Jackson, K. Spitler, M. F. Sharrock, C. M. Miller, C. Best, D. Llano, R. Du, *Front. Neurosci.* **2014**, *8*, 307.
- [77] F. Allab, A. Kedous-Lebouc, J. P. Yonnet, J. M. Fournier, *Int. J. Refrig.* **2006**, *29*, 1340.
- [78] A. M. Tishin, Y. I. Spichkin, V. I. Zverev, P. W. Egorf, *Int. J. Refrig.* **2016**, *68*, 177.
- [79] S. Zhang, Q. Yang, C. Li, Y. Fu, H. Zhang, Z. Ye, X. Zhou, Q. Li, T. Wang, S. Wang, W. Zhang, C. Xiong, Q. Wang, *Nat. Commun.* **2022**, *13*, 9.

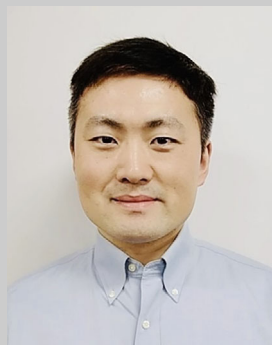
- [80] E. C. Davidson, A. Kotikian, S. Li, J. Aizenberg, J. A. Lewis, *Adv. Mater.* **2020**, *32*, 1905682.
- [81] J. Liu, T. Gottschall, K. P. Skokov, J. D. Moore, O. Gutfleisch, *Nat. Mater.* **2012**, *11*, 620.
- [82] S. A. Wilson, R. P. J. Jourdain, Q. Zhang, R. A. Dorey, C. R. Bowen, M. Willander, Q. U. Wahab, M. Willander, M. A. H. Safaa, O. Nur, E. Quandt, C. Johansson, E. Pagounis, M. Kohl, J. Matovic, B. Samel, W. van der Wijngaart, E. W. H. Jager, D. Carlsson, Z. Djinojic, M. Wegener, C. Moldovan, R. Iosub, E. Abad, M. Wendlandt, C. Rusu, K. Persson, *Mater. Sci. Eng., R.* **2007**, *56*, 1.
- [83] C. Cazorla, J. Íñiguez, *Phys. Rev. B.* **2018**, *98*, 174105.
- [84] S. Crossley, N. D. Mathur, X. Moya, *AIP Adv.* **2015**, *5*, 067153.
- [85] C. G. Granqvist, A. Hjortsberg, *J. Appl. Phys.* **1981**, *52*, 4205.
- [86] B. Zhao, W. J. Chen, J. H. Hu, Z. Y. Qiu, Y. G. Qu, B. B. Ge, *Energy Convers. Manage.* **2015**, *100*, 440.
- [87] R. Rajivgandhi, J. Aroust Chelvane, S. Quezado, S. K. Malik, R. Nirmala, *J. Magn. Magn. Mater.* **2017**, *433*, 169.
- [88] W. Park, H. Seo, J. Kim, Y. M. Hong, H. Song, B. J. Joo, S. Kim, E. Kim, C. G. Yae, J. Kim, J. Jin, J. Kim, Y. H. Lee, J. Kim, H. K. Kim, J. U. Park, *Nat. Commun.* **2024**, *15*, 2828.
- [89] S. Chen, N. Wu, S. Lin, J. Duan, Z. Xu, Y. Pan, H. Zhang, Z. Xu, L. Huang, B. Hu, J. Zhou, *Nano Energy.* **2020**, *70*, 104460.
- [90] S. Coyle, K. T. Lau, N. Moyna, D. O’Gorman, D. Diamond, F. Di Francesco, D. Costanzo, P. Salvo, M. G. Trivella, D. E. De Rossi, N. Taccini, *IEEE Trans. Inf. Technol. Biomed.* **2010**, *14*, 364.
- [91] G. Chen, X. Xiao, X. Zhao, T. Tat, M. Bick, J. Chen, *Chem. Rev.* **2022**, *122*, 3259.
- [92] Z. Wang, Y. Bo, P. Bai, S. Zhang, G. Li, X. Wan, Y. Liu, R. Ma, Y. Chen, *Science.* **2023**, *382*, 1291.
- [93] J. N. Munday, *Joule.* **2019**, *3*, 2057.
- [94] Y. Meng, Z. Zhang, H. Wu, R. Wu, J. Wu, H. Wang, Q. Pei, *Nat. Energy.* **2020**, *5*, 996.
- [95] Y. Liu, G. Lin, M. Medina-Sanchez, M. Guix, D. Makarov, D. Jin, *ACS Nano.* **2023**, *17*, 8899.
- [96] Y. Liu, M. Pharr, G. A. Salvatore, *ACS Nano.* **2017**, *11*, 9614.
- [97] C. Chen, Y. Liu, X. He, H. Li, Y. Chen, Y. Wei, Y. Zhao, Y. Ma, Z. Chen, X. Zheng, H. Liu, *Chem. Mater.* **2021**, *33*, 987.
- [98] M. Cianchetti, C. Laschi, A. Menciassi, P. Dario, *Nat. Rev. Mater.* **2018**, *3*, 143.
- [99] A. Esteva, A. Robicquet, B. Ramsundar, V. Kuleshov, M. DePristo, K. Chou, C. Cui, G. Corrado, S. Thrun, J. Dean, *Nat. Med.* **2019**, *25*, 24.
- [100] A. Aziz, S. Pane, V. Iacovacci, N. Koukourakis, J. Czarske, A. Menciassi, M. Medina-Sanchez, O. G. Schmidt, *ACS Nano.* **2020**, *14*, 10865.
- [101] N. Baghel, A. Kumar, *Solid State Sci.* **2025**, *160*, 107784.
- [102] S. Patel, Z. Rao, M. Yang, C. Yu, *Adv. Funct. Mater.* **2025**, *35*, 2417906.
- [103] H. Wang, Q. He, X. Gao, Y. Shang, W. Zhu, W. Zhao, Z. Chen, H. Gong, Y. Yang, *Adv. Mater.* **2024**, *36*, 2305453.
- [104] L. Jiang, D. Gan, C. Xu, T. Zhang, M. Gao, C. Xie, D. Zhang, X. Lu, *Small Sci.* **2025**, *5*, 2400362.
- [105] J. R. Sonawane, R. Jundale, A. A. Kulkarni, *Mater. Horiz.* **2025**, *12*, 364.
- [106] Z. Ye, T. Liu, G. Du, Y. Shao, Z. Wei, S. Zhang, M. Chi, J. Wang, S. Wang, S. Nie, *Adv. Funct. Mater.* **2025**, *35*, 2412545.
- [107] J. Zou, L. Tang, L. Kang, *ACS Nano.* **2025**, *19*, 152.
- [108] X. Zhao, G. Chen, Y. Zhou, A. Nashalian, J. Xu, T. Tat, Y. Song, A. Libanori, S. Xu, S. Li, J. Chen, *ACS Nano.* **2022**, *16*, 6013.
- [109] J. Xu, T. Tat, X. Zhao, Y. Zhou, D. Ngo, X. Xiao, J. Chen, *Appl. Phys. Rev.* **2022**, *9*, 031404.
- [110] Z. Che, X. Wan, J. Xu, C. Duan, T. Zheng, J. Chen, *Nat. Commun.* **2024**, *15*, 1873.
- [111] A. Libanori, J. Soto, J. Xu, Y. Song, J. Zarubova, T. Tat, X. Xiao, S. Z. Yue, S. J. Jonas, S. Li, J. Chen, *Adv. Mater.* **2023**, *35*, 2206933.
- [112] J. Xu, T. Tat, J. Yin, D. Ngo, X. Zhao, X. Wan, Z. Che, K. Chen, L. Harris, J. Chen, *Matter.* **2023**, *6*, 2235.
- [113] R. Finster, P. Sankaran, E. Bihar, *Adv. Electron. Mater.* **2025**, *11*, 2400763.
- [114] M. U. Khalid, A. Rudokaite, A. M. H. Silva, M. Kirsnyte-Snioke, A. Stirke, W. C. Melo, *Nanomaterials.* **2025**, *15*, 106.
- [115] Z. Lin, J. Yang, X. Li, Y. Wu, W. Wei, J. Liu, J. Chen, J. Yang, *Adv. Funct. Mater.* **2018**, *28*, 1704112.
- [116] K. Meng, X. Xiao, W. Wei, G. Chen, A. Nashalian, S. Shen, X. Xiao, J. Chen, *Adv. Mater.* **2022**, *34*, 2109357.
- [117] Y. Zhou, X. Xiao, G. Chen, X. Zhao, J. Chen, *Joule.* **2022**, *6*, 1381.
- [118] T. Tat, G. Chen, X. Zhao, Y. Zhou, J. Xu, J. Chen, *ACS Nano.* **2022**, *16*, 13301.



Xiujun Fan is currently a Ph.D. student in the Department of Bioengineering at the University of California, Los Angeles, under the supervision of Prof. Jun Chen. Her research focuses on developing soft bioelectronics for personalized healthcare. She is the first author of a journal article published in *Proceedings of the National Academy of Sciences of the United States of America*.



Songyue Chen is a Ph.D. student in the Department of Bioengineering at the University of California, Los Angeles, under the supervision of Prof. Jun Chen. His research focuses on developing soft bioelectronics for healthcare applications. He has published five journal articles, including four as the first author in *Nature Nanotechnology*, *Matter*, *Biomaterials*, and *Materials Science and Engineering: R: Reports*.



Jun Chen is currently an associate professor with tenure in the Department of Bioengineering at the University of California, Los Angeles (UCLA). His research focuses on soft matter innovation for healthcare and energy. He has published 2 books and 380 journal articles, with 280 of them being corresponding authors and a current *h*-index of 125. Among his many accolades are the V. M. Watanabe Excellence in Research Award (1 faculty per year in UCLA Samueli School of Engineering), Shu Chien Early Career Award, MRS Outstanding Early-Career Investigator Award, Advanced Materials Rising Star, among others.